JOURNAL OF GEOPHYSICAL RESEARCH, VOL. 108, NO. D13, 4383, doi:10.1029/2002JD002993, 2003

A stratospheric aerosol climatology from SAGE II and CLAES measurements: 2. Results and comparisons, 1984–1999

J. J. Bauman and P. B. Russell
NASA Ames Research Center, Moffett Field, California, USA

M. A. Geller
State University of New York, Stony Brook, New York, USA

Patrick Hamill
San Jose State University, San Jose, California, USA

Received 27 September 2002; accepted 28 February 2003; published 8 July 2003.

[1] This paper presents a climatology of the stratospheric aerosol produced with our look-up table (LUT) technique using data from the Stratospheric Aerosol and Gas Experiment (SAGE II) and the Cryogenic Limb Array Etalon Spectrometer (CLAES) instruments. The LUT climatology spans the period from December 1984 to August 1999. It includes values and uncertainties of measured extinction and optical depth at four SAGE II wavelengths (0.385–1.02 μm) and supplements these with results from the CLAES 12.82 μm wavelength during the key period January 1992 through May 1993, when the large particle sizes from the Pinatubo volcanic injection made many SAGE II extinction and optical depth spectra wavelength independent. Also included are retrieved values of effective radius R_{eff}, distribution width σ_g, surface area S, and volume V. Aerosol retrievals show notable increases in all these parameters after major volcanic eruptions, with increases in R_{eff} lagging increases in the others. Postvolcanic increases in σ_g, indicative of broader size distributions, are consistent with sudden increases in numbers of both small and large particles that exceed increases in intermediate-size particles. After Pinatubo, retrieved R_{eff} and σ_g took nearly 5 years to return to pre-eruption values, while slightly shorter recovery times were obtained for S and V. During low-aerosol-loading periods, size distributions narrow in going from the tropical core to higher latitudes at altitudes between 20 and 22 km. Seasonal variations in S and V are observed at high latitudes for several altitude bands, but are less obvious in R_{eff}. With some exceptions, LUT retrievals agree well with most previous climatologies. For example, agreement is good between LUT retrieved surface area and results from balloon-borne measurements, where available. However, there are a few noteworthy discrepancies. For example, values of surface area from principal component analysis of SAGE II data are less than LUT retrievals during near-background periods (e.g., 1989 to mid-1991, and after 1996) and greater than LUT retrievals in the peak of the Pinatubo plume. The smaller LUT-derived surface areas during the Pinatubo peak result from the constraint provided by the CLAES 12.82 μm extinction measurements. *INDEX TERMS:* 0305 Atmospheric Composition and Structure: Aerosols and particles (0345, 4801); 0340 Atmospheric Composition and Structure: Middle atmosphere—composition and chemistry; 0370 Atmospheric Composition and Structure: Volcanic effects (8409); 0394 Atmospheric Composition and Structure: Instruments and techniques; 3309 Meteorology and Atmospheric Dynamics: Climatology (1620); *KEYWORDS:* stratospheric aerosols, volcanic aerosol and climate response, aerosol-climate interaction, effective radius, SAGE II, CLAES

Citation: Bauman, J. J., P. B. Russell, M. A. Geller, and P. Hamill, A stratospheric aerosol climatology from SAGE II and CLAES measurements: 2. Results and comparisons, 1984–1999, *J. Geophys. Res.*, *108*(D13), 4383, doi:10.1029/2002JD002993, 2003.

1. Introduction

[2] In spite of the recent upsurge of research into the nature of stratospheric aerosols, our understanding of the potential influence of these particles on climate modifica-

0148-0227/03/2002JD002993$09.00

tion is still far from complete, and is hampered by inadequacies of existing data sets and a paucity of aerosol observations that are spatially and temporally comprehensive. In view of their climatic importance, a continuous global data set of stratospheric aerosols is essential to better understand the role they play in atmospheric chemistry, dynamics, radiation and climate. This task requires information regarding the spatiotemporal distribution of wavelength-dependent aerosol extinction and optical depth, as well as key particle size descriptors, surface area, and volume: a suite of information rarely, if ever, available.

[3] The goal of this paper is to describe the optical and physical properties of the stratospheric aerosol. We have produced a global climatology of the stratospheric aerosol using data from the Stratospheric Aerosol and Gas Experiment (SAGE II) and the Cryogenic Limb Array Etalon Spectrometer (CLAES) instruments. This paper describes the spatial and temporal characteristics of these properties, presents explanations of the major results, where possible, and compares our climatology with previous climatologies that have appeared in the literature. We presented a detailed discussion of the methodology used to generate this climatology in a companion paper [*Bauman et al.*, 2003] (hereinafter referred to as paper 1).

[4] Our climatology includes values and uncertainties of measured extinction and optical depth at four SAGE II wavelengths (0.385, 0.453, 0.525 and 1.02 μm) and, for the period January 1992 through May 1993, at the CLAES wavelength 12.82 μm. Also included are retrieved particle effective (area weighted) radius R_{eff}, distribution width σ_g, surface area S, volume V, and their uncertainties. Retrieved aerosol parameters are zonally averaged in 1 month × 5° latitude × 1 km altitude sampling bins. The climatology spans nearly 15 years, from December 1984 to August 1999. This time frame encompasses the El Chichón recovery period, a period of several smaller volcanic eruptions, a two to three year low-optical-depth period beginning in 1989, the June 1991 eruption of Mount Pinatubo, three to four years of post-Pinatubo aerosol dissipation, and approximately 3 years of low aerosol optical depth from 1996 to 1999.

[5] In this paper we begin by illustrating results of aerosol physical parameters retrieved from SAGE II and CLAES optical measurements using the LUT technique (section 2). In section 3, we present a description of the measured optical properties, including aerosol extinction and integrated optical depth, followed by a discussion in section 4 of the retrieved microphysical properties, including effective radius, size distribution width, particle surface area and volume. Explanation of observed spatial and temporal variability in aerosol retrievals is given where possible. In section 5 we compare our climatology with previously published climatologies.

2. Illustrative Results: Retrieving Physical Parameters From Optical Measurements

[6] Examples of SAGE II and CLAES measured optical properties with corresponding LUT retrievals of R_{eff}, S and V are shown in Figure 1. Included are vertical profiles of aerosol extinction and column integrated optical depths from the near-ultraviolet to the infrared. Example extinction profiles and uncertainties are presented in the top row in Figure 1 for seven sample months (indicated at the top of each frame) in the 15–20°N latitude band. Each colored profile is for a given SAGE II or CLAES wavelength. Horizontal dashed lines in each frame mark the height of the tropopause. The second row shows a time series of optical depths for the entire 15-year data record in the 15–20°N latitude band. Optical depths are computed from extinction profiles by integrating upward from 2 km above the tropopause to an altitude of 40.5 km. All column-integrated properties (i.e., optical depth, column R_{eff}, S and V) during SAGE II saturation (e.g., in January 1992 below 22 km) are based on estimates of extinction at the SAGE II wavelengths using the methods of L. W. Thomason (NASA Langley Research Center, personal communications, 1999). Vertical red lines mark the eruptions of Ruiz, Kelut and Pinatubo, while shading highlights the months sampled in row 1. Optical depth spectra for the seven sample months are shown in row 3 (left scale). The black horizontal lines are retrieved values of R_{eff} (right scale) based on the sample spectra. The fourth row presents a time series of column R_{eff} (left scale), S and V (right scale) retrieved by the LUT from optical depth values in row 2. The last row presents profiles and uncertainties of retrieved R_{eff} (bottom scale), S and V (top scale) for the seven sample months in rows 1 and 3.

[7] Relatively large extinction values ($\beta > 10^{-3}$ km^{-1}) in the January 1985 profiles (row 1, Figure 1) between 19 and 26 km indicate that the stratosphere was still recovering from the April 1982 eruption of El Chichón at that time. Error bars increase above about 27 km, where SAGE II data are of poorer quality because of reduced aerosol concentration, which causes an increase in the relative contribution from Rayleigh scattering, and O_3 and NO_2 absorption. Five months prior to the Pinatubo eruption, in January 1991, extinction profiles show little evidence of a well-defined stratospheric aerosol layer peak. Instead, extinction measurements decrease monotonically with altitude above the tropopause and do not exceed 10^{-3} km^{-1}. At this time the stratospheric aerosol appears to be near "background" levels. The aerosol particles exhibit a relatively small retrieved value of $R_{eff} = 0.22$ μm. The associated SAGE II extinction spectrum in January 1991 decreases monotonically with wavelength, with the largest extinction measured at the shortest SAGE II wavelength, 0.385 μm.

[8] Immediately after the Pinatubo eruption in July 1991, the situation is quite different, as illustrated in Figure 1. Extinction measurements at all wavelengths increase sharply below 27 km, indicating the vertical extent of the aerosol cloud between 15 and 20°N. Error bars on extinction values below this altitude approach 100%. These "error bars" are actually a combination of the SAGE II archived extinction measurement uncertainty and the extinction variability in a time-latitude-altitude bin (paper 1). The relatively large error bars are in this case caused by large spatial variability. Large error bars on the extinction values are propagated to large error bars on retrieved effective radius, as seen in retrievals in rows 4 and 5. The peak in the measured extinction spectrum shifts to longer wavelengths, from 0.385 μm prior to Pinatubo to 0.525 μm in July 1991. Correspondingly, derived values of R_{eff}, S and V increase markedly relative to pre-eruption values. Over the next year and a half, until January 1993, the extinction spectra in the SAGE II wavelength range are spectrally flat (i.e., independent of wavelength) within error bars. Such flat spectra are consistent

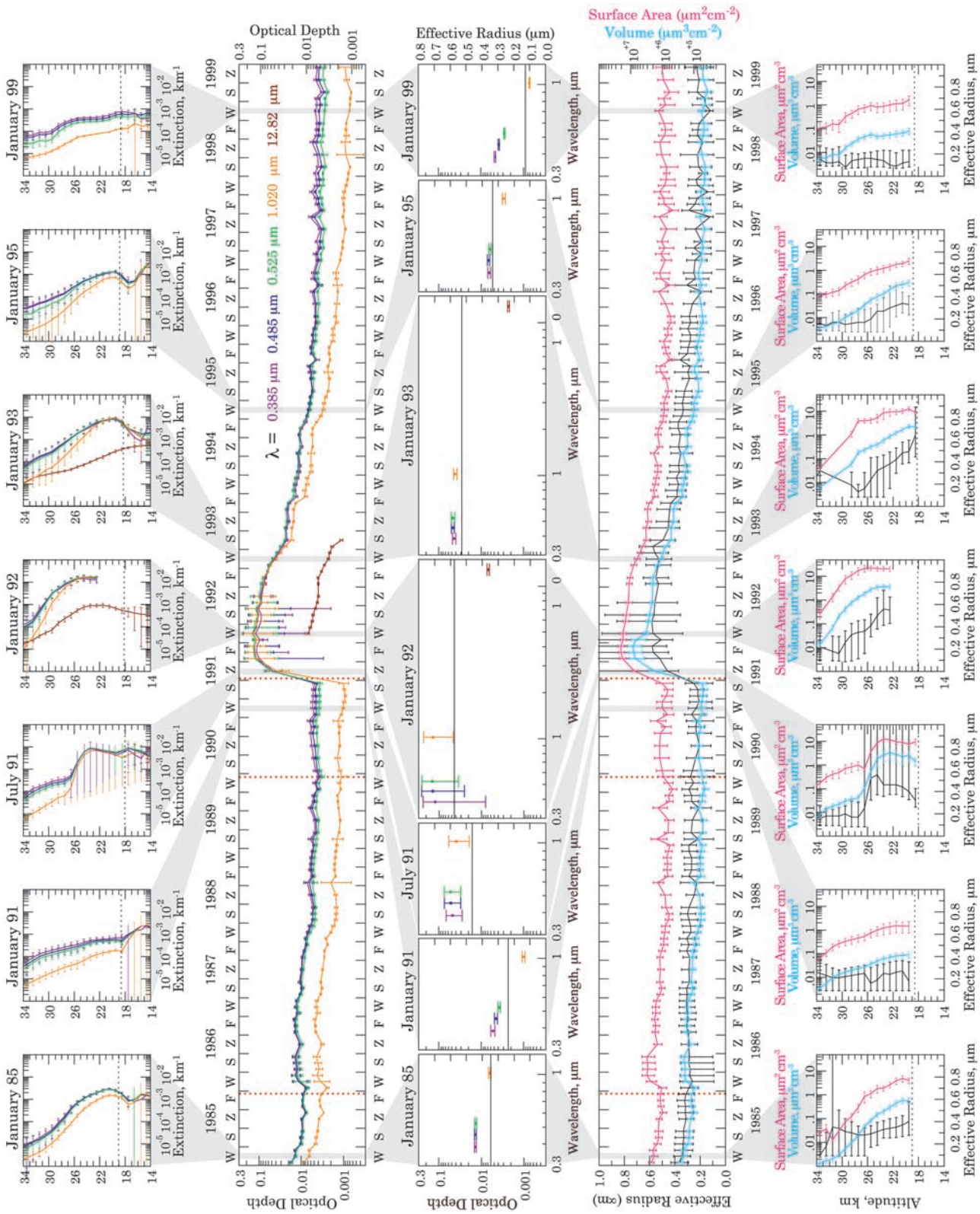

Figure 1. Row 1: SAGE II and CLAES measured extinction profiles and error bars in the 15–20°N latitude band for seven sample months indicate at the top of each frame. Dotted lines mark the tropopause. Row 2: Time series of integrated optical depths from December 1984 to August 1999. Dotted red lines mark the eruptions of Ruiz (Nov. 1985), Kelut (Feb. 1990) and Pinatubo (Jun. 1991). Vertical shading highlights the months sampled in rows 1, 3 and 5. Row 3: Profiles of retrieved R_{eff} (right scale). Row 4: Time series of retrieved column integrated R_{eff} (left scale), S and V (top scale) for the months in rows 1 and 3. Dotted lines mark the tropopause.

with effective radii of about 0.5 μm or larger, as noted by retrievals in row 4. Hence upper error bars on retrievals of R_{eff} are unbounded from the first month following Pinatubo until January 1992, when CLAES infrared extinction measurements become available. It is interesting to note that the peak in retrieved R_{eff} lags behind the peaks in both optical depth (at all wavelengths) and retrieved surface area and volume density. For example, while values of S and V reach a maximum in Fall 1991 and decline thereafter, associated retrievals of R_{eff} display a broad peak between Fall 1991 and Winter 1992. It is likely that during this period growth by condensation and coagulation (which tends to increase R_{eff}) outweighed or balanced preferential loss of larger particles by sedimentation (which tends to decrease R_{eff}).

[9] After approximately January 1993, the visible to near-IR extinction spectra in the 15–20°N latitude band begin to peak at progressively shorter wavelengths, indicating the start of a return toward pre-Pinatubo spectral shapes. Concurrently, column estimates of R_{eff} begin to decay slowly toward pre-eruption values (see rows 3 and 4). The January 1992, 1993 and 1995 extinction profiles show a gradual decline in the altitude of the Pinatubo plume peak with time. For example, over this 3 year period, the altitude of the 0.385 μm extinction maximum fell nearly 6 km, from 25 to 19 km. Peaks in retrieved aerosol parameters, while not as well-defined as peaks in extinction, similarly subsided with time as a result of gravitational settling. The time series in row 4 shows that it took nearly 5 years, until mid-1996, for particle effective radius to return to pre-Pinatubo values, with slightly shorter recovery times for surface area and volume. By January 1999, the stratospheric aerosol had reached record low values of both the measured optical and retrieved physical parameters.

3. Measured Optical Properties

3.1. Aerosol Extinction

[10] The magnitude and wavelength dependence of globally measured extinction are key descriptors of aerosol evolution and dispersion. Zonal averages of extinction at each of the SAGE II and CLAES wavelengths used in this study are shown in Figures 2 through 6. Measurements are presented as a function of latitude and time at eight altitudes between 16.5 and 30.5 km. Saturation of SAGE II tropical measurements occurred within one to two months following the Pinatubo eruption at altitudes below 24 km. Dark regions appearing at 16.5 and 18.5 km, but not at higher altitudes, are below the 'tropopause plus 2 km' criterion and are not considered here.

[11] Perturbations caused by the eruptions of Ruiz, Kelut and Pinatubo (marked by the letters "R", "K" and "P", respectively) are clearly evident at all altitudes. An exception is the February 1990 eruption of Kelut, whose influence extends only to about 24 km. Enhanced extinction at all SAGE II wavelengths is also observed in 1985, which is attributable to the remnants of the 1982 eruption of El Chichón. There tends to be a monotonic decrease in extinction values following each indicated eruption in the record. With the exception of Pinatubo, the decline toward pre-eruption values is interrupted by subsequent eruptions. It is likely that minimum equilibrium extinction values were never attained prior to Pinatubo. This pattern was noted in studies by *McCormick and Veiga* [1992] and by *Hitchman et al.* [1994]. This suggests that complete decay of volcanically enhanced aerosol to a "background aerosol" may occur infrequently. Hitchman et al. point out that the volcanic activity experienced from 1979 to 1990 is broadly representative of the volcanic activity noted over the past century. Thus it is likely that the stratospheric aerosol layer is frequently volcanic in nature. Most observed increases in aerosol extinction that occur several kilometers above the tropopause over an extended period (excluding polar stratospheric clouds (PSCs)) can be traced to a volcanic origin.

3.2. Aerosol Optical Depth

[12] SAGE II column integrated optical depths at four wavelengths are presented in Figure 7, which shows the impact of volcanoes on the stratospheric aerosol. A seasonal fluctuation in optical depth at high latitudes is superimposed on the posteruption decay of aerosol loading throughout the data record. Enhanced optical depths at high latitudes may occur in response to particle formation over the polar regions (PSCs) during local winter in both hemispheres. However, PSC formation generally takes place at latitudes greater than 70° within the polar vortex. Therefore the seasonal variation is more likely related to seasonal variations in tropopause height and to the fact that particles exposed to colder environments will absorb water and grow larger [*Steele and Hamill*, 1981].

[13] Inspection of Figure 7 reveals the tendency for latitudinal banding in values of optical depth, a pattern noted during both volcanically influenced and near-background periods. Maximum optical depth occurs within the tropics and at high latitudes, while minimum values are found between latitudes of approximately 15° and 45°. This feature was discussed in papers by *Kent and McCormick* [1984], *McCormick and Wang* [1987], and *Trepte et al.* [1994]. The low-latitude maximum arises from the "aerosol reservoir" over the tropics, identified by *Trepte and Hitchman* [1992]. Episodic transport of stratospheric air into the troposphere through tropopause folds coincides with observed midlatitude minima in zonal mean optical depth. *Trepte et al.* [1994] pointed out that tropopause folds are not necessary to account for the observed banded pattern in stratospheric aerosol optical depths. They argue that the high-latitude maximum is a consequence of the departure of the tropopause from isentropic surfaces. This results in accumulation of aerosols in the lower stratosphere that have been transported from lower latitudes. This reasoning is in accord with the Brewer-Dobson circulation in the lower stratosphere: rising motion in the tropics, subsidence at high latitudes, and a net poleward flow in midlatitudes [*Brewer*, 1949; *Dobson*, 1956]. Transport of aerosol to lower altitudes causes an increase in aerosol density due to compression; this suggests that a large portion of the enhanced optical depths at high latitude may arise from this increase in aerosol density. Two alternative explanations for the observed high-latitude optical depth maximum are offered in the following section.

4. Retrieved Microphysical Properties

4.1. Effective Radius

[14] The particle effective radius, or area-weighted radius, is a useful parameter in the description of a particle size

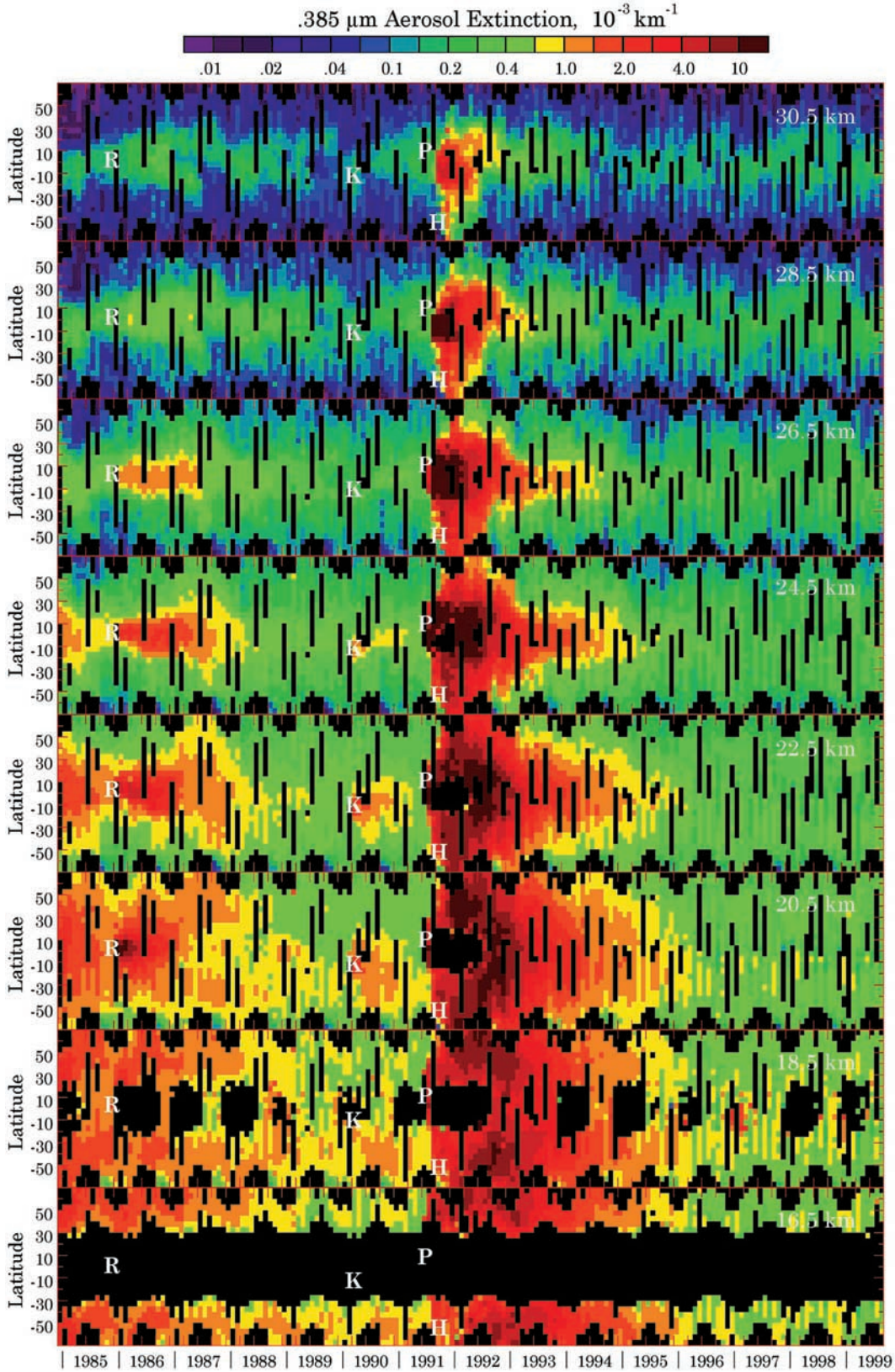

Figure 2. Zonally averaged 0.385 μm aerosol extinction at 30.5, 28.5, 26.5, 24.5, 22.5, 20.5, 18.5 and 16.5 km. The letters repeated in each frame mark the latitude and time of the Ruiz (R), Kelut (K), Pinatubo (P) and the Hudson (H) eruptions.

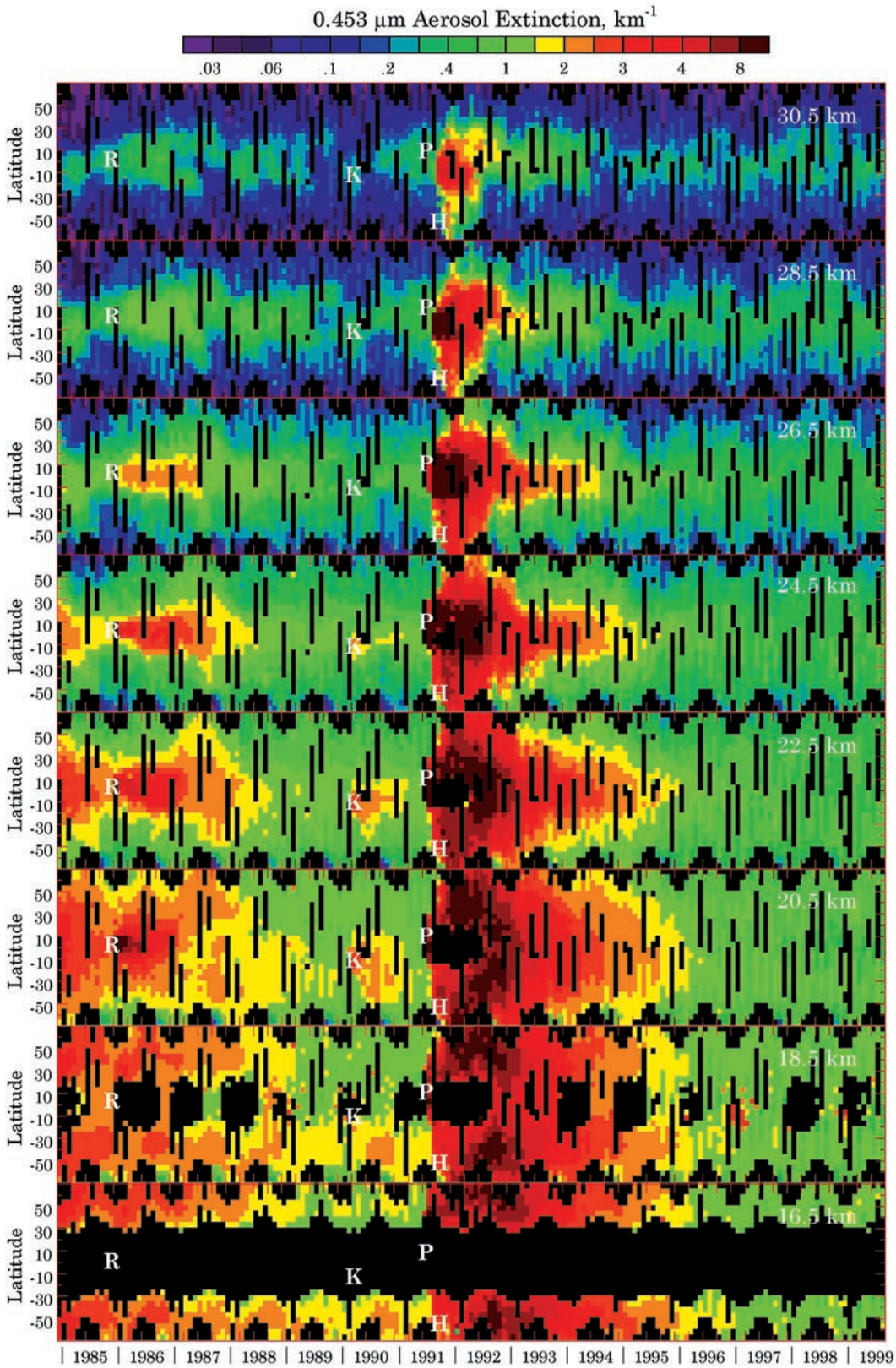

Figure 3. Zonally averaged 0.453 μm aerosol extinction at 30.5, 28.5, 26.5, 24.5, 22.5, 20.5, 18.5 and 16.5 km. The letters repeated in each frame mark the latitude and time of the Ruiz (R), Kelut (K), Pinatubo (P) and the Hudson (H) eruptions.

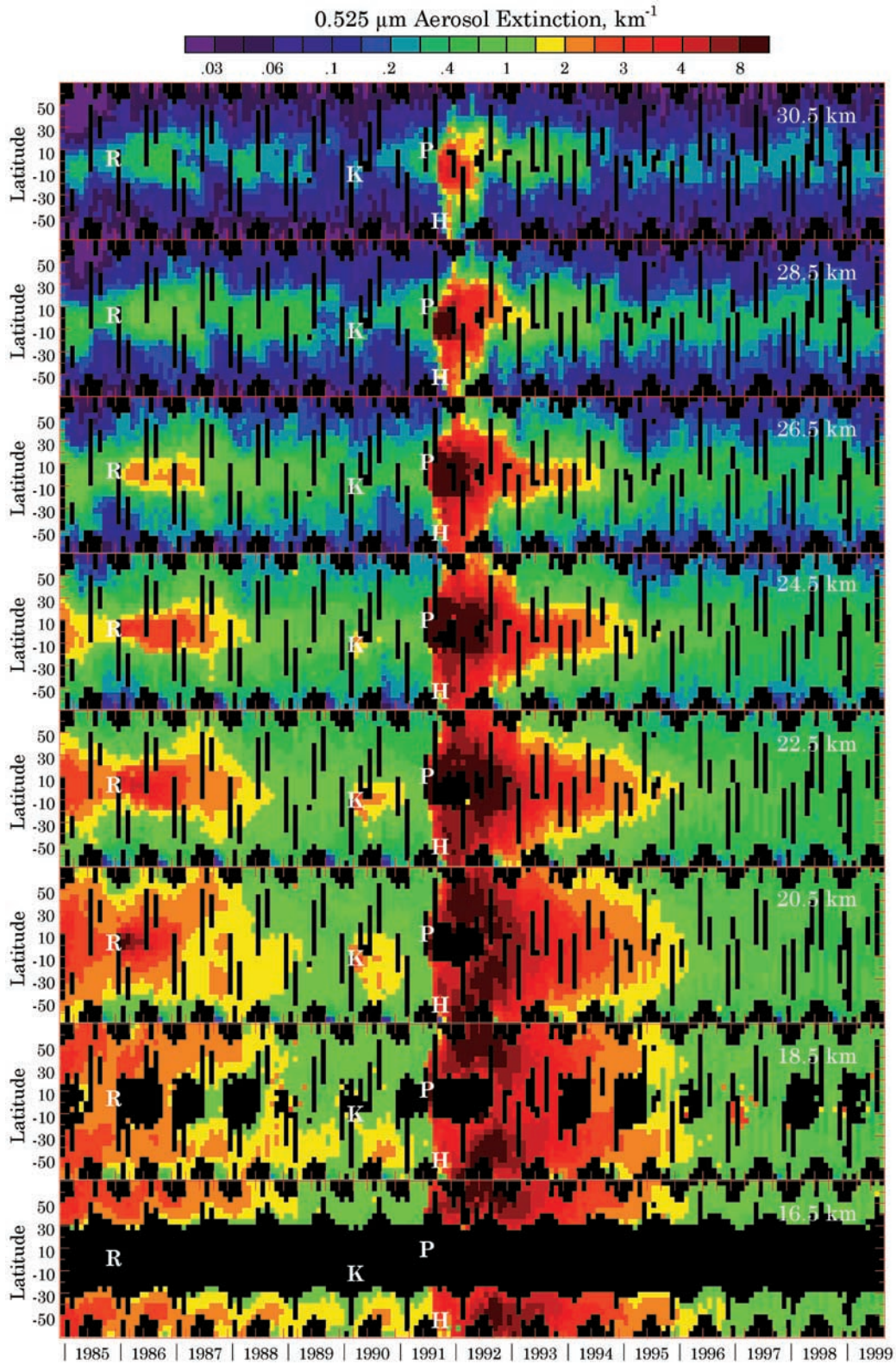

Figure 4. Zonally averaged 0.525 μm aerosol extinction at 30.5, 28.5, 26.5, 24.5, 22.5, 20.5, 18.5 and 16.5 km. The letters repeated in each frame mark the latitude and time of the Ruiz (R), Kelut (K), Pinatubo (P) and the Hudson (H) eruptions.

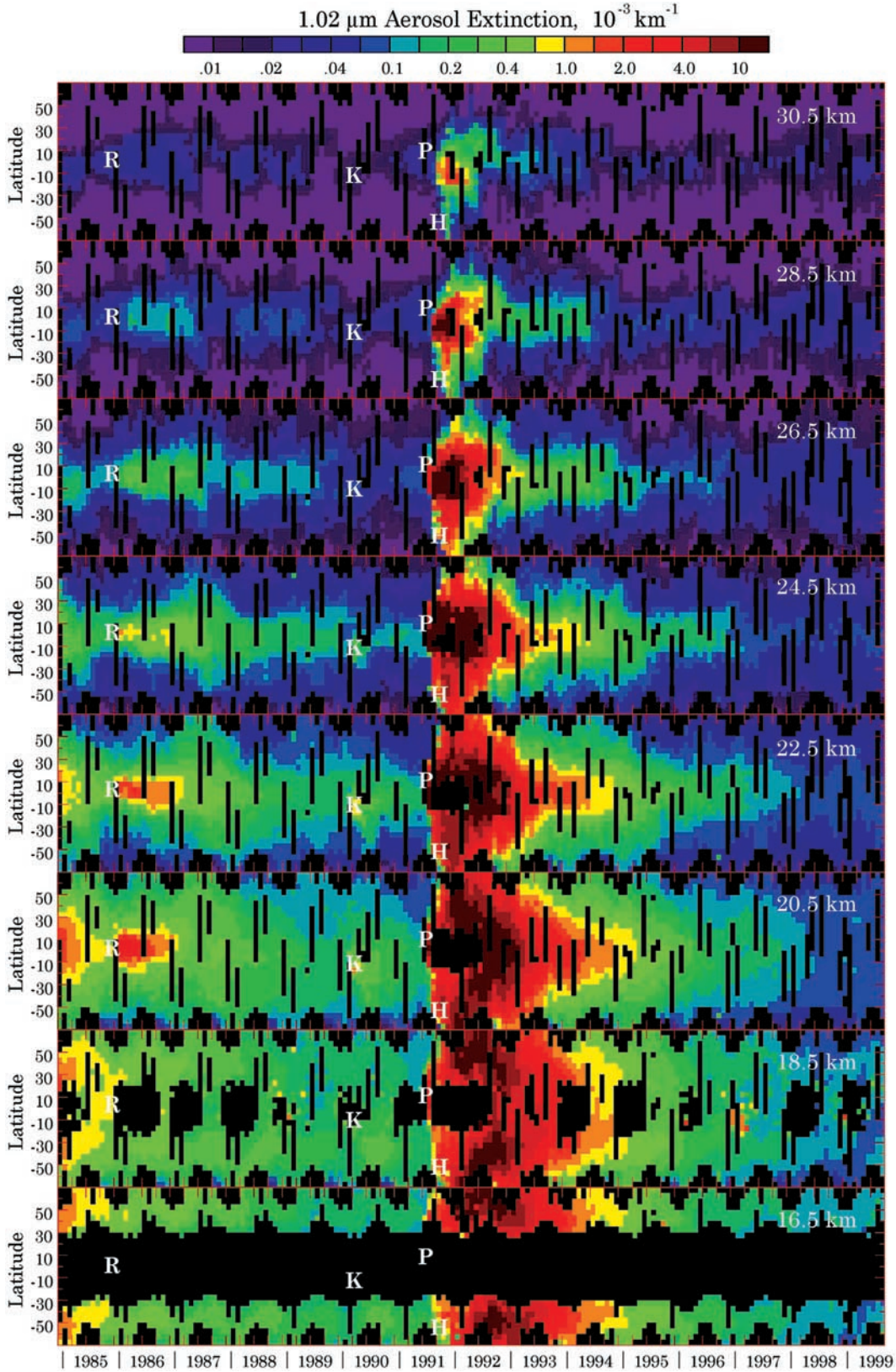

Figure 5. Zonally averaged 1.02 μm aerosol extinction at 30.5, 28.5, 26.5, 24.5, 22.5, 20.5, 18.5 and 16.5 km. The letters repeated in each frame mark the latitude and time of the Ruiz (R), Kelut (K), Pinatubo (P) and the Hudson (H) eruptions.

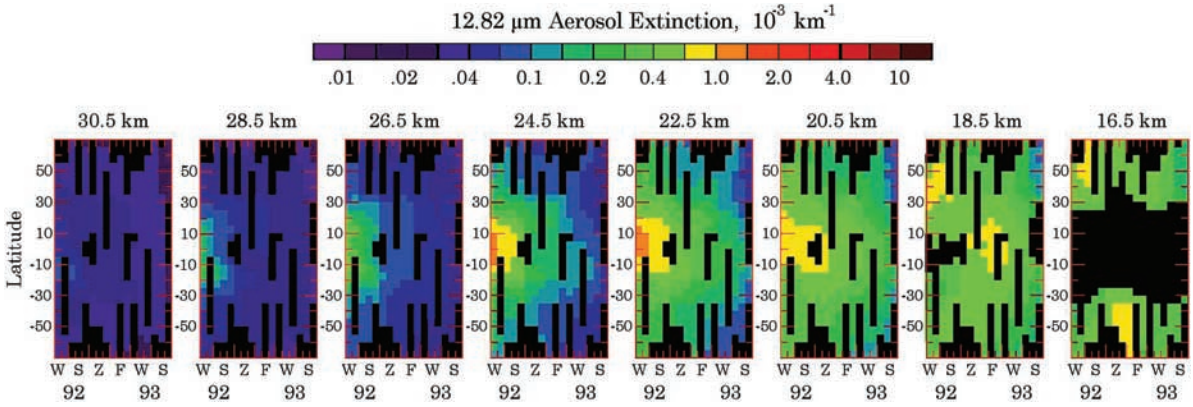

Figure 6. Zonal-averaged 12.82 μm extinction at 30.5, 28.5, 26.5, 24.5, 22.5, 20.5, 18.5 and 16.5 km.

distribution. The evolution of the size distribution at a fixed latitude and altitude depends on several factors, including: (1) condensation and coagulation (which tend to increase R_{eff}); (2) evaporation (which tends to decrease R_{eff}); (3) gravitational sedimentation (which tends to remove larger particles faster and hence reduce R_{eff}); and (4) transport from other locations (which either increases or decreases R_{eff}). The variation of R_{eff} with time is thus an indicator of the microphysical processes taking place in the atmosphere. Zonal mean distributions of retrieved effective radius are shown in Figure 8 as a function of latitude and time for seven altitudes from 18.5 to 30.5 km. During the January 1992 to May 1993 period, CLAES extinction data were available and were used in this study. Although this 15 month period is short compared to the ~15 year period of this study, it makes a key contribution because the flat extinction spectra from SAGE II (0.385–1.02 μm) in 1992 and early 1993 gave no upper bound on R_{eff} (see paper 1).

[15] Figure 9 shows altitude-latitude cross sections of seasonally averaged R_{eff} for the 15-year data record: from

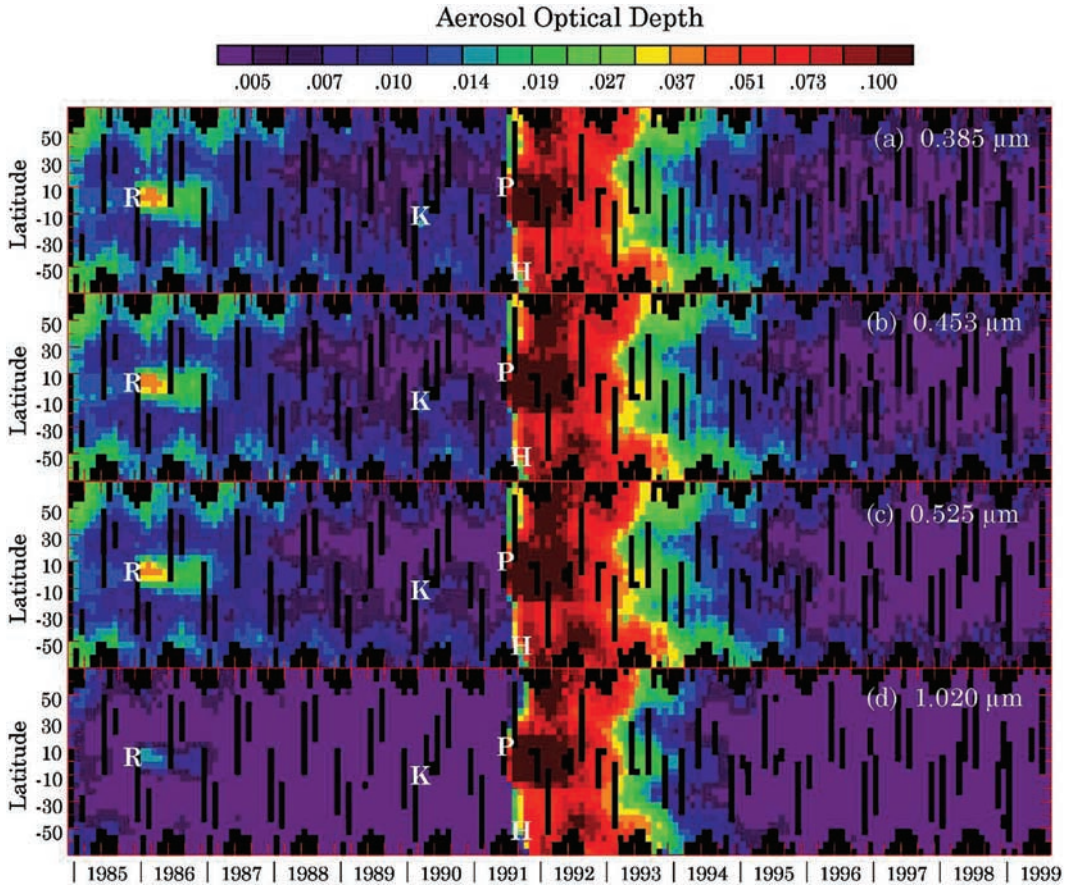

Figure 7. Latitude-time cross sections of zonally averaged aerosol optical depth at (a) 0.385 μm, (b) 0.453 μm, (c) 0.525 μm, and (d) 1.02 μm. The letters repeated in each frame mark the latitude and time of the Ruiz (R), Kelut (K), Pinatubo (P) and the Hudson (H) eruptions.

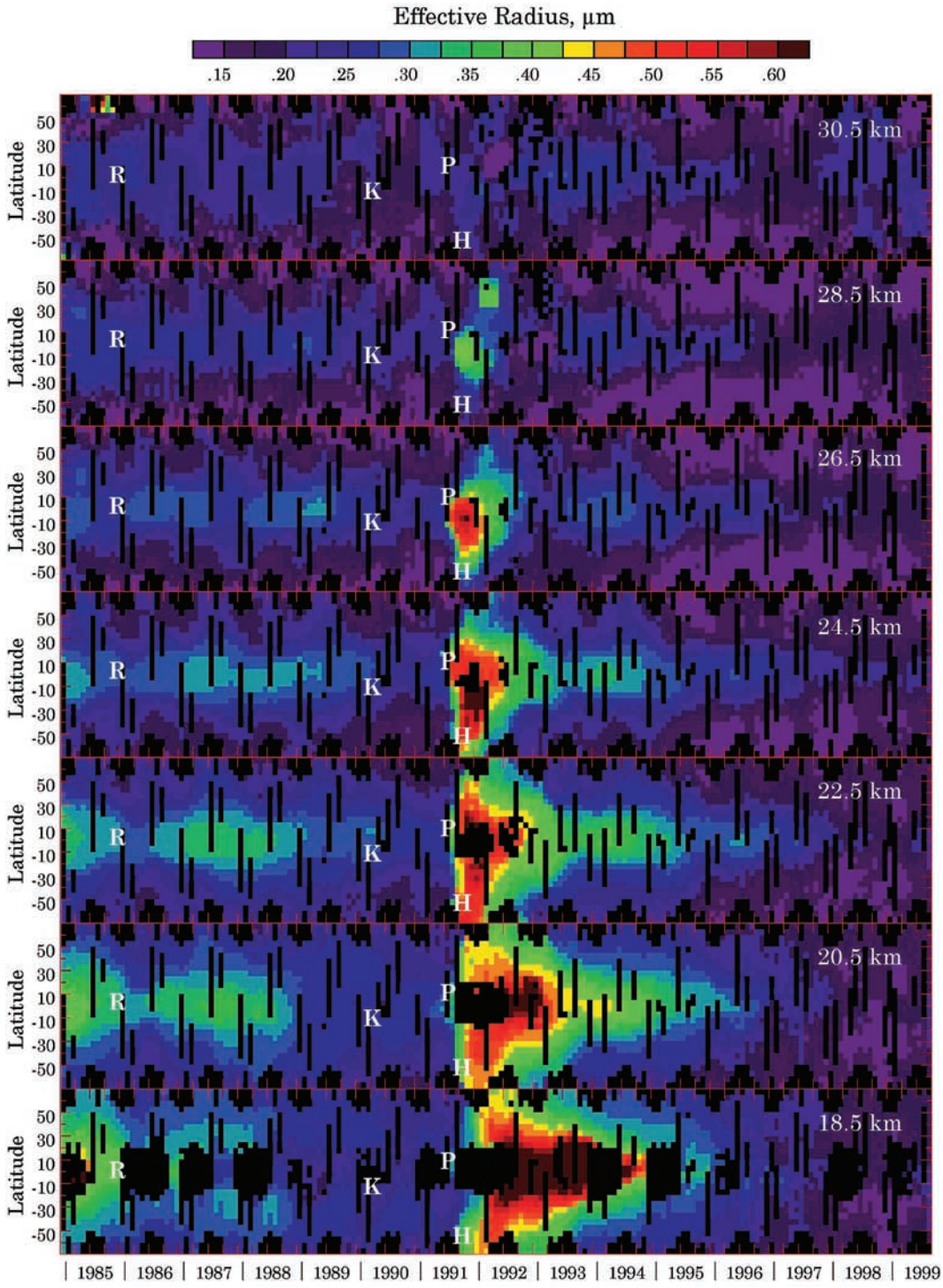

Figure 8. Latitude-time cross-sections of retrieved aerosol effective radius R_{eff} at 18.5, 20.5, 22.5, 24.5, 26.5, 28.5 and 30.5 km. The letters repeated in each frame mark the latitude and time of the Ruiz (R), Kelut (K), Pinatubo (P) and the Hudson (H) eruptions.

Winter (DJF) 1985 to Summer (JJA) 1999. It is interesting to note that values of effective radius evolve differently with respect to altitude after the eruptions of Ruiz, Kelut and Pinatubo. For example, the figure shows that following the Pinatubo eruption (Summer 1991) there was a layer of large particles extending from just above the tropical tropopause at 18.5 km up to about 25 km. The effective radius at 18.5 km displayed a broad peak that persisted for nearly 3 years, until June 1994, and declined thereafter. Maximum values of R_{eff} reached 0.6 μm or greater. At progressively higher altitudes, the duration of the effective radius peak shortened in time. Because of SAGE II saturation, it is not possible to define the time of maximum effective radius below approximately 24 km. The peak in R_{eff} near 26.5 km was short-lived, with a maximum value of 0.6 μm occurring in the 5–10°S latitude band during October 1991. Following

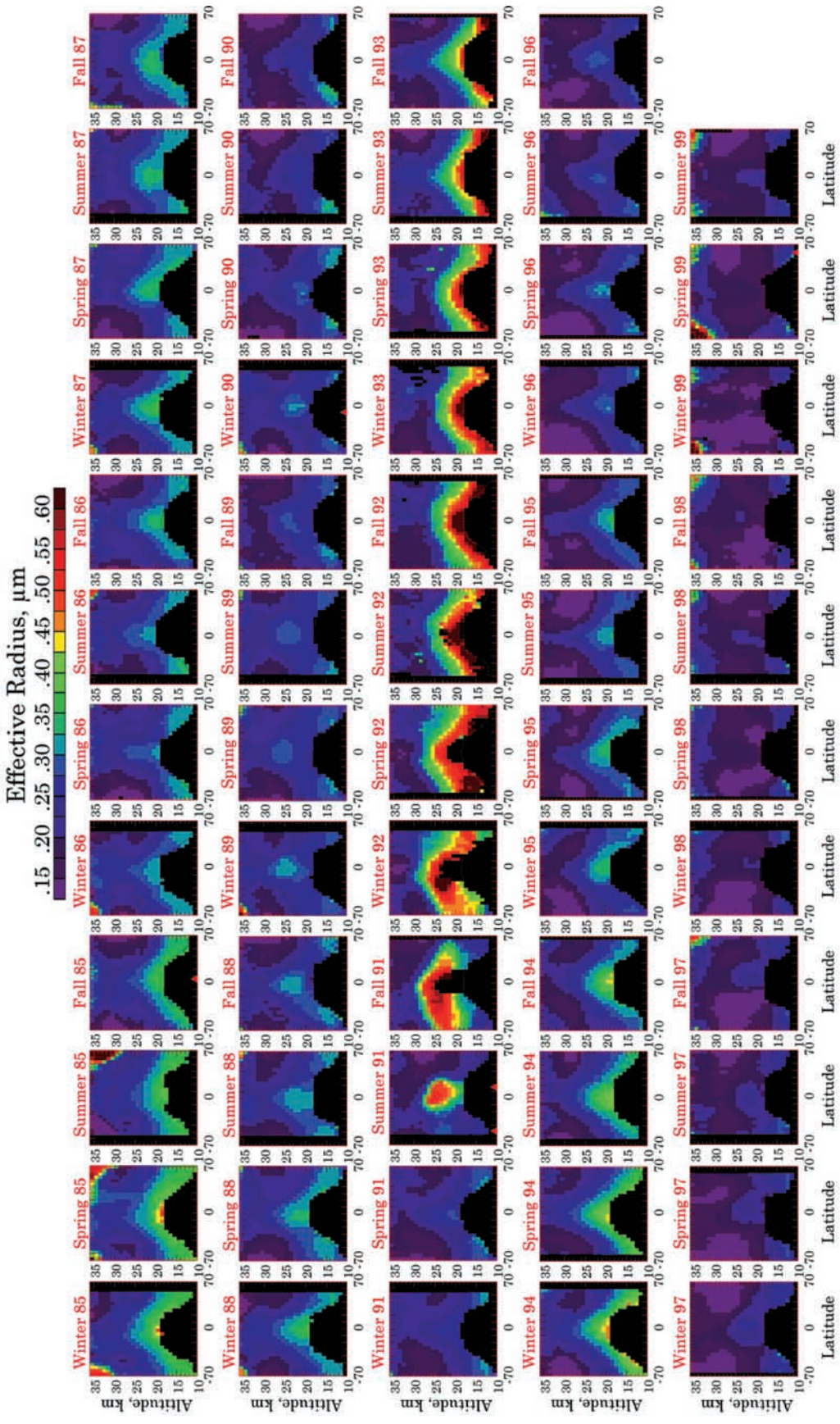

Figure 9. Seasonally averaged retrieved R_{eff}, Winter (DJF) 1985 to Summer(JJA) 1999.

Table 1. Location, Date of Eruption, and Estimated SO_2 Loading of Major Volcanic Eruptions That Occurred Between 1982 and 1999[a]

Volcano	Latitude	Longitude	Eruption Date	SO_2(Mt)	Reference
El Chichon	17.3 N	93.2 W	Apr 1982	8–12	1
Nevado del Ruiz	4.9 N	75.3 W	Nov 1985	0.5	2
Kelut	7.9 S	112.3 E	Feb 1990	0.3	3
Pinatubo	15.2 N	120.3 E	Jun 1991	14–30	4
Cerro Hudson	45.9 S	72.9 W	Aug 1991	3	5
Shishaldin	54.8 N	164.0 W	Apr 1999	–	–

[a]Note that no estimate of SO_2 loading is available for Shishaldin. References: 1, *Russell et al.* [1996] and *Evans and Kerr* [1983]; 2, *Krueger et al.* [1990]; 3, *Bluth et al.* [1997]; 4, *Russell et al.* [1996] and *Bluth et al.* [1992]; and 5, *Doiron et al.* [1991].

the eruption of Ruiz (November 1985), the duration of the peak in effective radius is also negatively correlated with altitude. However, the onset of peak R_{eff} values tends to be positively correlated with altitude. That is, values of effective radius peaked later in time at successively higher altitudes. For example, at 20.5 km, peak R_{eff} values of $\sim$0.35 μm occurred between six months and two and a half years after Ruiz in the tropics. At 26.5 km, there is a short-lived tropical peak in R_{eff} of slightly smaller magnitude from January to May 1989, nearly three and a half years after Ruiz. Finally, Figures 8 and 9 show that the effects of the February 1990 eruption of Kelut on effective radius were hardly apparent at the lowest altitudes (above 18.5 km) and not apparent at all at the highest altitudes.

[16] Of the four factors affecting the evolution of size distribution mentioned above, it is likely that the distinct patterns in effective radius with altitude noted after Ruiz and Pinatubo are due to differences in either condensation/coagulation growth rates, sedimentation rates or a combination thereof. For example, larger particles have faster sedimentation rates. Differences in retrieved particle size noted in Figure 8 after each eruption should lead to faster sedimentation rates following Pinatubo (relative to Ruiz). Over time, the relative concentration of larger particles at higher altitudes, where fall-speed is the greatest, is quickly reduced as a result of gravitational settling. This could explain in part the three-year difference in timing of peak effective radius between Ruiz and Pinatubo at high altitudes. However, we caution that R_{eff}, the area-weighted radius, is not the same as an effective sedimentation radius, which can be strongly influenced by the largest particles.

[17] Faster sedimentation after Pinatubo than after Ruiz would be consistent with the idea that larger volcanic eruptions have a greater potential to quickly clear the stratosphere of aerosol particles. Such a mechanism was proposed by *Pinto et al.* [1989], who suggested that larger eruptions (like Pinatubo) create larger particles. This is consistent with estimates of SO_2 loading given in Table 1 and the values of R_{eff} in Figure 8. It is unclear at this point why values of R_{eff} should peak so late at high altitudes following Ruiz.

4.2. Size Distribution Width

[18] The particle size distribution width or standard deviation, σ_g, varies as a result of aerosol formation and evolutionary processes. The LUT algorithm can retrieve some information about distribution width by noting the range of σ_g values for which computed extinction spectra are consistent with SAGE II and CLAES measurements. A given value of σ_g is consistent with measurements if the LUT is able to retrieve a range of R_{eff} for which the calculated extinction spectrum satisfies the χ^2 criterion (equation (7b) of paper 1).

[19] For several months preceding the eruption of Pinatubo only small values of σ_g are consistent with measurements. To quantify this statement, we resolved the measurement latitudes into 28 bins between 70°S and 70°N with each bin spanning 5 degrees and determined the set of consistent distribution widths for each bin.

[20] Figure 10 is a time series of the weighted mean of the distribution widths defined by

$$\frac{\sum_{\sigma_g} \sigma_g n_{\sigma_g}}{\sum_{\sigma_g} n_{\sigma_g}} \tag{1}$$

where n_{σ_g} is the number of latitude bins in which a given σ_g is allowed. At most altitudes, the mean distribution width declined gradually from 1985 to early spring 1991. This decline is followed by a sharp increase in σ_g values in June 1991. By the end of 1992, the mean distribution widths begin to decline toward pre-eruption values. However, at 24.5 km the mean σ_g value took nearly six years to return to the pre-Pinatubo value of 1.7. Following the Pinatubo eruption, the sharpest increases in σ_g occur in the peak of the aerosol plume, between 20.5 and 26.5 km. At altitudes above 30.5 km, no significant variation is noted in the mean distribution width with time.

[21] The above estimates of σ_g are zonal means averaged over all latitudes (i.e., global averages). Figure 11 presents latitudinally dependent retrievals of size distribution width at seven altitudes between 30.5 and 18.5 km. At most altitudes, wide distribution widths ($\sigma_g \geq 2.4$) are noted immediately after the eruptions of Ruiz, Kelut and Pinatubo (marked by the letters "R", "K" and "P", respectively). Immediate postvolcanic size distributions are broader than prevolcanic distributions due to sudden increases in both smaller and larger particles. *Russell et al.* [1996] noted that the greatest relative increases in particle number concentration after the Pinatubo eruption occurred for the smallest and largest sizes. This was also observed immediately after the eruption of El Chichón by *Hofmann and Rosen* [1983]. It is likely that the smaller particles are freshly nucleated sulfuric acid solution droplets [*Hofmann and Rosen*, 1983; *Deshler et al.*, 1992], whereas the larger particles may be ash fragments injected into the stratosphere at all altitudes.

[22] Approximately six months after the initial increase, values of σ_g in the peak of the Ruiz and Pinatubo plumes decline sharply in the tropics to approximately 1.4 or less. Figure 11 shows that tropical values of σ_g six months to four years after Pinatubo are often less than pre-eruption values. During this period, narrow distribution widths are also noted at higher latitudes below the aerosol layer peak. To a first approximation, values of σ_g in Figure 11 tend to be negatively correlated with retrieved values of R_{eff} shown in Figure 8 from about June 1986 to December 1988, and from about January 1992 to January 1995. *Hervig et al.* [1998] state that small values of σ_g are characteristic of large-particle ensembles. They argue that according to condensa-

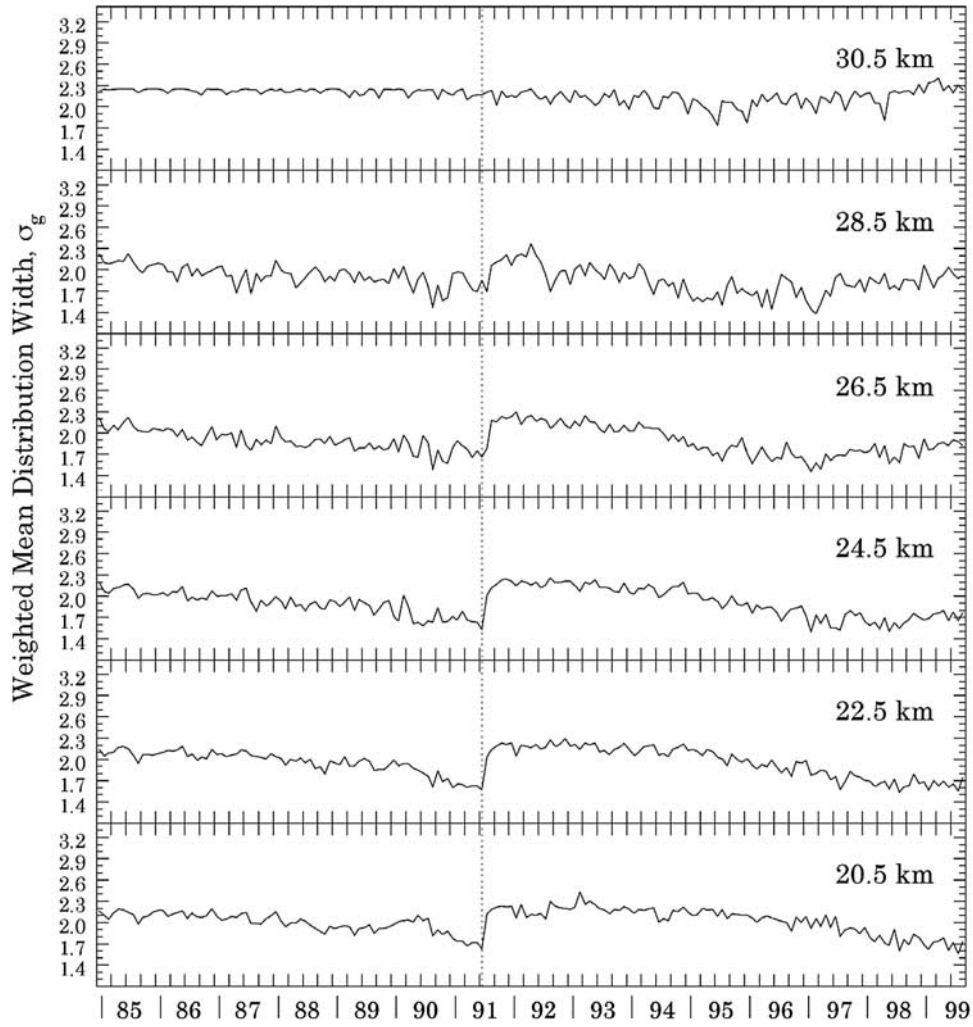

Figure 10. Time series of global weighted mean width σ_g at 30.5, 28.5, 26.5, 24.5, 22.5 and 20.5 km. The vertical dashed line marks the Pinatubo eruption.

tional growth theory [*Pruppacher and Klett*, 1980], the growth rate of a solution droplet increases with decreasing radius. Thus smaller particles grow faster, resulting in narrowing distributions during particle growth. Particle sedimentation enhances this narrowing, because larger particles are removed faster than smaller ones. Results of *Hamill et al.* [1977] show that in the stratosphere the growth rate is inversely proportional to particle size only for particles greater than approximately 0.2 μm radius and for smaller particles the growth rate (dr/dt) is independent of particle radius. Figure 8 shows that particle sizes frequently exceed this size limit in the aftermath of Ruiz and Pinatubo. Thus the theory of Hervig et al. may in part explain the narrow distribution widths noted in the tropics six months to several years after the Ruiz and Pinatubo eruptions. As can be appreciated from the expression for the lognormal size distribution (see paper 1) the quantity σ_g is a measure of the relative width of the size distribution. That is, for a given σ_g the width of the size distribution is proportional to the geometric mean radius r_g.

[23] To interpret the decline in tropical values of σ_g six months to several years after the Ruiz and Pinatubo eruptions it is important to keep in mind that retrievals by the LUT are based on a unimodal lognormal distribution. In paper 1 we show that if the particle size distribution is large-mode-dominant bimodal, then the LUT retrieved unimodal distribution tends to match the larger mode fairly well, but fails to account for the smaller particles in the first mode. Following Pinatubo, aerosol distributions were often large-mode-dominant bimodal. Thus as particles grow, it is the width of the larger mode that narrows in Figure 10 from January 1992 to January 1995. Over time, particle distributions tend to evolve from large-mode-dominant to small-mode-dominant bimodal (or unimodal). The LUT retrieved unimodal size distribution then widens as it shifts toward smaller particle sizes in an attempt to fit both modes of the distribution. This may account for the subsequent return to larger values of σ_g in the tropics immediately following the period of narrow distribution widths (e.g., in mid-1995 between 20 and 24 km).

[24] During near-background periods from January 1989 to May 1991, and after approximately 1996, Figure 11 shows that size distribution widths narrow with time at all latitudes and altitudes. Narrow distribution widths are often

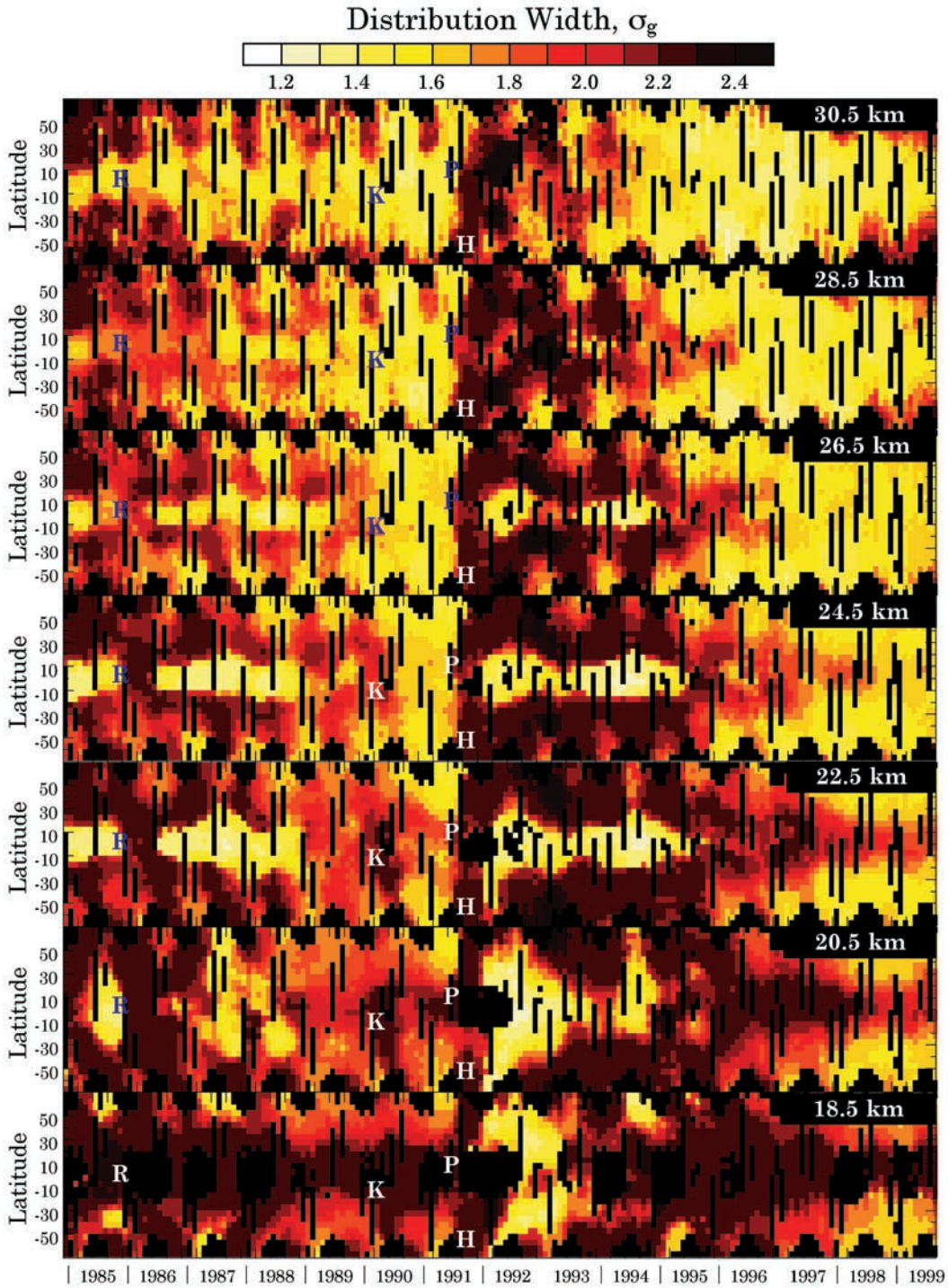

Figure 11. Retrieved size distribution width σ_g as a function of latitude and time at 30.5, 28.5, 26.5, 24.5, 22.5, 20.5 and 18.5 km. The letters repeated in each frame mark the latitude and time of the Ruiz (R), Kelut (K), Pinatubo (P) and the Hudson (H) eruptions.

an indicator of aged aerosols. It is generally thought that freshly nucleated particles grow through condensation and coagulation, and larger particles settle out. Over time, this leads to narrow distributions with small- to intermediate-sized particles. As the geometric mean radius diminishes, changes in σ_g are positively correlated with changes in R_{eff}. This is consistent with decreasing values of R_{eff} obtained during these periods (compare Figure 8). Declining values of σ_g are also evident in the global averages presented in Figure 10.

4.3. Surface Area and Volume Density

[25] Column retrievals of stratospheric aerosol effective radius, surface area and volume are shown in Figure 12 as a function of latitude and time. There are several noteworthy differences between retrievals of R_{eff} and retrievals of S and

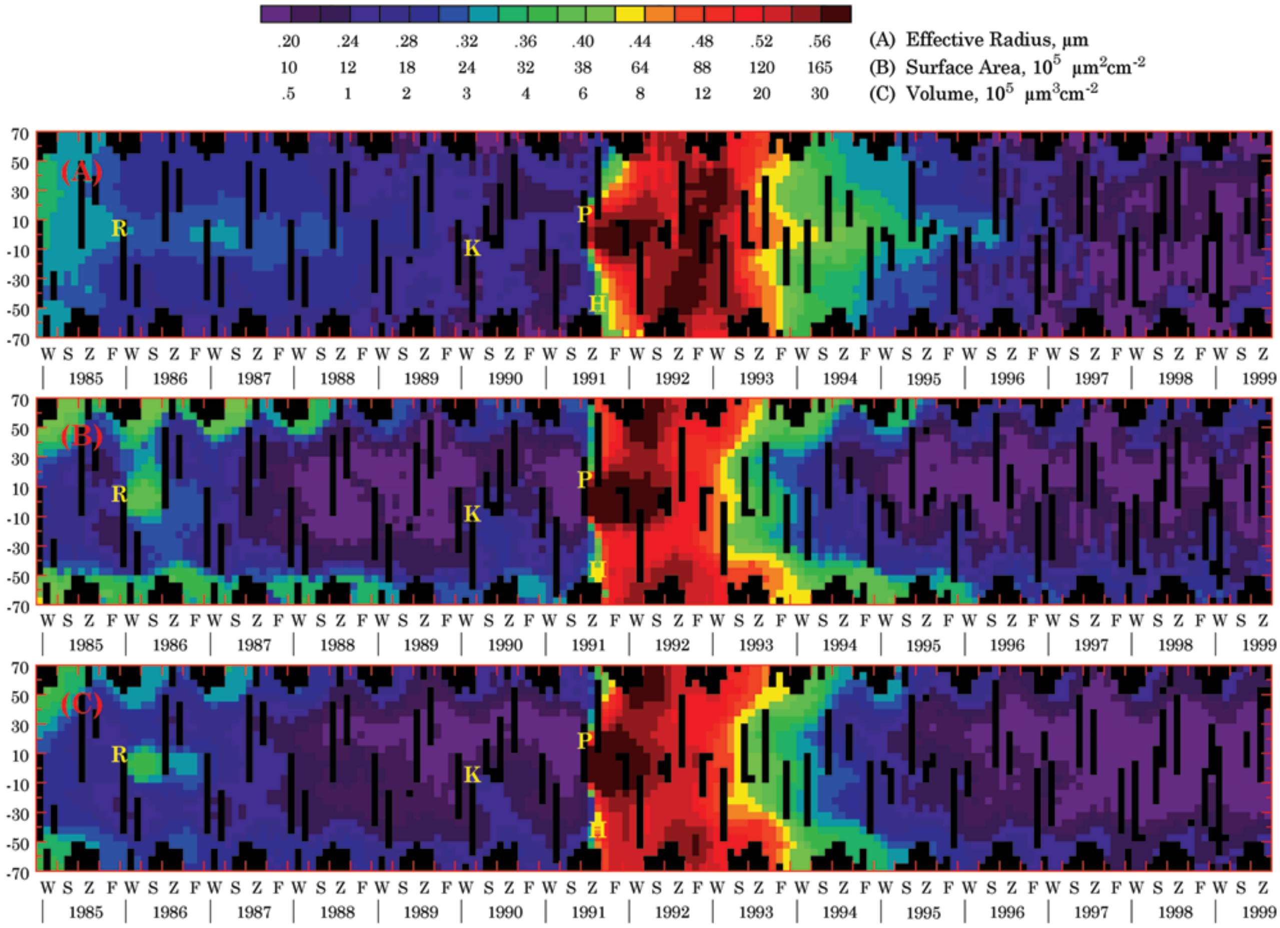

Figure 12. LUT retrieved values of (a) column effective radius R_{eff}, (b) column surface area S, and (c) column volume V as a function of latitude and time. The letters repeated in each frame mark the latitude and time of the Ruiz (R), Kelut (K), Pinatubo (P) and the Hudson (H) eruptions.

V. For example, while all retrievals show notable increases after Ruiz and Pinatubo, the effects of the relatively small eruption of Kelut are not as apparent in R_{eff} as they are in S and V. There are periods in the data record (e.g., 1994–1995) when R_{eff} decreases toward higher latitudes, while positive gradients in S and V are observed between the equator and high latitudes. This typically occurs when the stratospheric aerosol is volcanic in nature and well dispersed (e.g., from 1988 to 1989, and from 1995 to 1996). The figure shows that it took nearly a year after the eruption of Ruiz for column estimates of R_{eff} to reach peak values of $\sim$0.33 µm, while values of S and V peaked within 3 months at 4×10^6 µm^{2}cm^{-3} and 5×10^5 µm^{3}cm^{-3}, respectively. Following the eruption of Pinatubo, peaks in R_{eff} similarly lag peaks in S and V at most latitudes. Several similarities in retrieval patterns are also apparent in the figure. For example, after the eruption of Pinatubo, R_{eff}, S and V peak progressively later at higher latitudes. The initial increase at midlatitudes to high latitudes tends to occur after the initial decline in tropical values of R_{eff}, S and V. This suggests that the time delay in peaking at higher latitudes is likely due to poleward transport of particles from the tropical reservoir rather than in situ growth by condensation and coagulation.

[26] As with the optical depth shown in Figure 7, a seasonal fluctuation in S and V at high latitudes is superimposed on the posteruption decay throughout the data record. Although not as obvious, this pattern is also noted in retrievals of column R_{eff} during near-background periods. Seasonal variations are emphasized in Figure 13, which shows time series of column volume density (top frame) and surface area density (bottom frame) between December 1984 and May 1991 for the 50–55°N and the 50–55°S latitude bands. Gray regions highlight winter-spring (summer-fall) in the northern (southern) hemisphere. Seasonal extremes in retrievals of both S and V are most pronounced in the northern hemisphere.

[27] Figures 14 and 15 show zonal mean distributions of retrieved surface area and volume as a function of latitude and time for seven altitudes from 18.5 to 30.5 km. The recovery of the lower stratosphere from the El Chichón eruption is most notable in retrievals of S at higher latitudes from 1984 to mid-1991. During this period estimates of S decrease from 5 to 1 µm^{2}cm^{-3} at 18.5 km. From mid-1991 to the end of 1995 values of S and V are dominated by the eruption of Pinatubo, particularly at lower altitudes. The impact of Kelut is evident at altitudes as high as 24 km, while the influence of the Cerro Hudson eruption in August 1991 is difficult to separate from that of Mount Pinatubo above 18.5 km. Following the eruption of Ruiz, values of S and V reach a maximum near 20 km. There are some

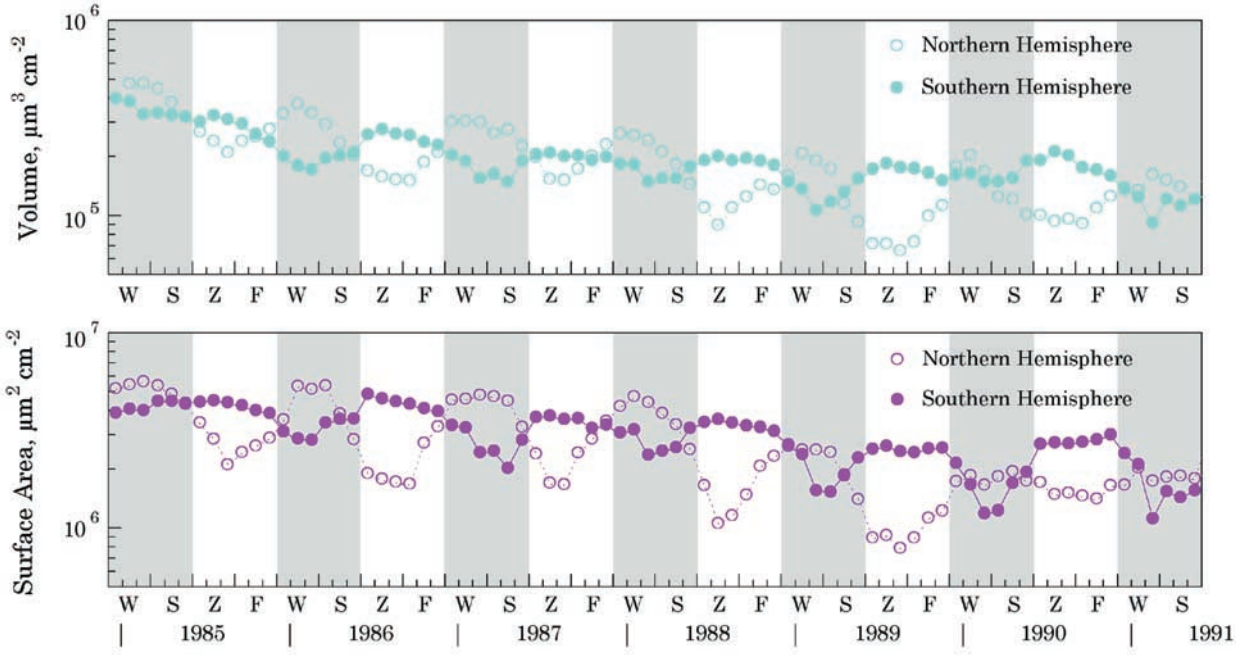

Figure 13. Time series of column volume density (top frame) and surface area density (bottom frame) between December 1984 and May 1991 for 50–55°N and 50–55°S. Gray bands highlight winter-spring (summer-fall) in the northern (southern) hemisphere.

discernible differences between the evolution of R_{eff} and the evolution of S and V following Ruiz. As shown in Figure 8, the duration of the peak effective radius is negatively correlated with altitude, and the onset of peak R_{eff} values occurs later at higher altitudes. Neither of these two features are noted in the structures of S and V in Figures 14 and 15. The peaks in S and V tend to occur within 3 months of Ruiz and persist from 4 months to 1 year. Following the eruption of Pinatubo, maximum values of S and V occur at higher altitudes, near 26 km, between 2 and 6 months after the eruption, and exceed 25 $\mu m^2 cm^{-3}$ and 8 $\mu m^3 cm^{-3}$, respectively. As described by *Young et al.* [1994], aerosol-induced heating at lower altitudes during late 1991 was sufficient to loft aerosol to higher altitudes and promote subsequent transport to southern latitudes (but not significantly to northern latitudes). This is made evident by elevated aerosol levels at 30.5 km, which are temporary phenomena associated with the Pinatubo eruption. In tropical and southern latitudes, S and V at 30.5 km increased by a factor of 10 or more (e.g., S increased from about 0.2 to 4 $\mu m^2 cm^{-3}$, while V increased from about 0.03 to 0.3 $\mu m^3 cm^{-3}$ in southern midlatitudes).

[28] The seasonal evolution of stratospheric aerosol surface area and volume over the 15-year period from Winter 1985 to Summer 1999 is illustrated by the zonal mean distributions shown in Figures 16 and 17. The figures show that the cloud from the Ruiz eruption (triangle, Fall 85) was largely confined to the tropics, while the aerosol from the Kelut eruption (triangle, Winter 89) spread rapidly to high southern latitudes. This is seen most clearly in retrievals of aerosol surface area (Figure 16). One possible explanation for the difference in transport is the shear phase of the quasi-biennial oscillation (QBO), which controls meridional mixing. That is, tropical aerosols tend to be confined to the tropics during periods in which an easterly shear is the dominant phase of the QBO [*Hitchman et al.*, 1994]. Poleward spreading occurs more readily during QBO westerly shear. (A period of easterly shear is one with easterly wind speed increasing with altitude, e.g., easterlies above westerlies in the region of interest: in this case the tropics from the tropopause up to ~35 km. Conversely, when westerlies are above easterlies, the shear is westerly.) An easterly QBO shear prevailed in the tropics above 21 km at the time of the Pinatubo eruption. This may have inhibited poleward spreading above this altitude in Summer 1991, as suggested by steep meridional gradients in retrievals of S and V in the subtropics. However, Figures 16 and 17 show that by Fall 1991 a substantial part of the aerosol cloud had spread to high latitudes in both hemispheres despite a persisting easterly shear. The rapid latitudinal transport may be a result of circulation setup by aerosol-induced lower stratospheric heating, as mentioned by *Young et al.* [1994]. During Fall 1991 the bulk of the aerosol cloud was distributed asymmetrically about the equator, with the largest values of surface area and volume located between 5°S and 20°N near 24 to 28 km. However, values of S and V as great as 10 $\mu m^2 cm^{-3}$ and 4 $\mu m^3 cm^{-3}$, respectively, extended southward to 55°S. The portion of the aerosol cloud with the largest values of S and V north of 30°N was located below 18.5 km, where transport occurred in association with the Asian monsoon [*McCormick et al.*, 1993].

[29] In the southern hemisphere during the few months following Pinatubo, the polar vortex boundary blocked meridional transport of Pinatubo aerosol to high latitudes until the vortex dissipated in November 1991. In contrast, stratospheric aerosol from the eruption of Cerro Hudson was concentrated at altitudes below 15 km (i.e., largely below the vortex) and penetrated deeply into high southern

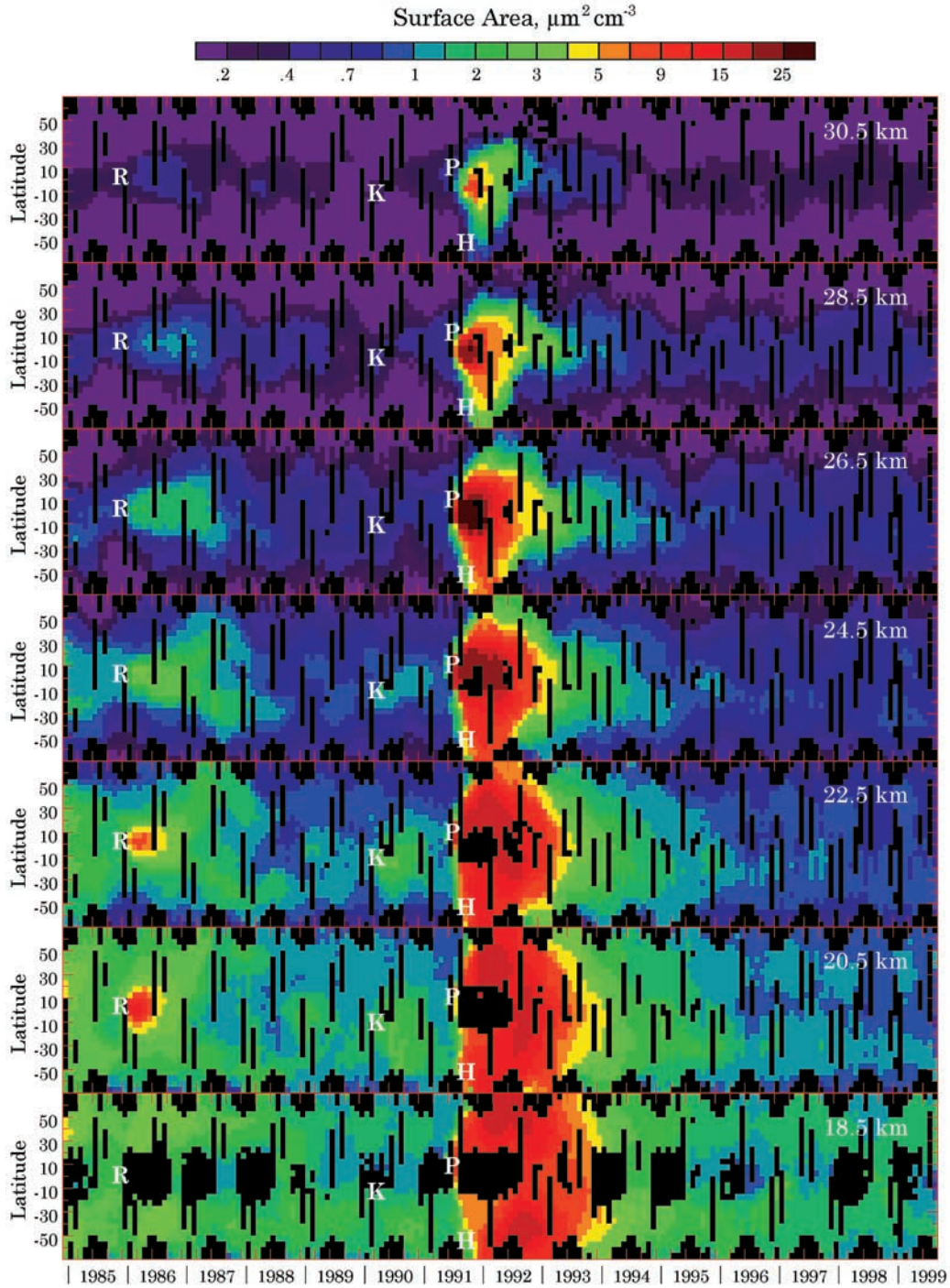

Figure 14. Latitude-time cross-sections of LUT-retrieved aerosol surface area density S at 18.5, 20.5, 22.5, 24.5, 26.5, 28.5 and 30.5 km. The letters repeated in each frame mark the latitude and time of the Ruiz (R), Kelut (K), Pinatubo (P) and the Hudson (H) eruptions.

latitudes soon after the eruption. Figures 16 and 17 show a clear separation of the Hudson and Pinatubo clouds in Fall 1991, which was not discernable in previous figures. *Deshler et al.* [1992] noted O_3 decreases of 50% between 11 and 13 km in the month following the arrival of Hudson aerosol over Antarctica. Until that time, O_3 loss had not been observed below the base of the vortex (~14 km). Aerosol surface area density in this layer during Fall 1991 is approximately 20 $\mu m^2 cm^{-3}$. This is 10 times that observed in Fall 1990 at the same location. By Spring 1992, the Hudson and Pinatubo clouds are difficult to distinguish in retrievals of S and V.

5. Comparisons

[30] We now present direct comparisons of the LUT climatology to several different climatologies, including: (1) *Deshler et al.* [1993], who presented a time history of

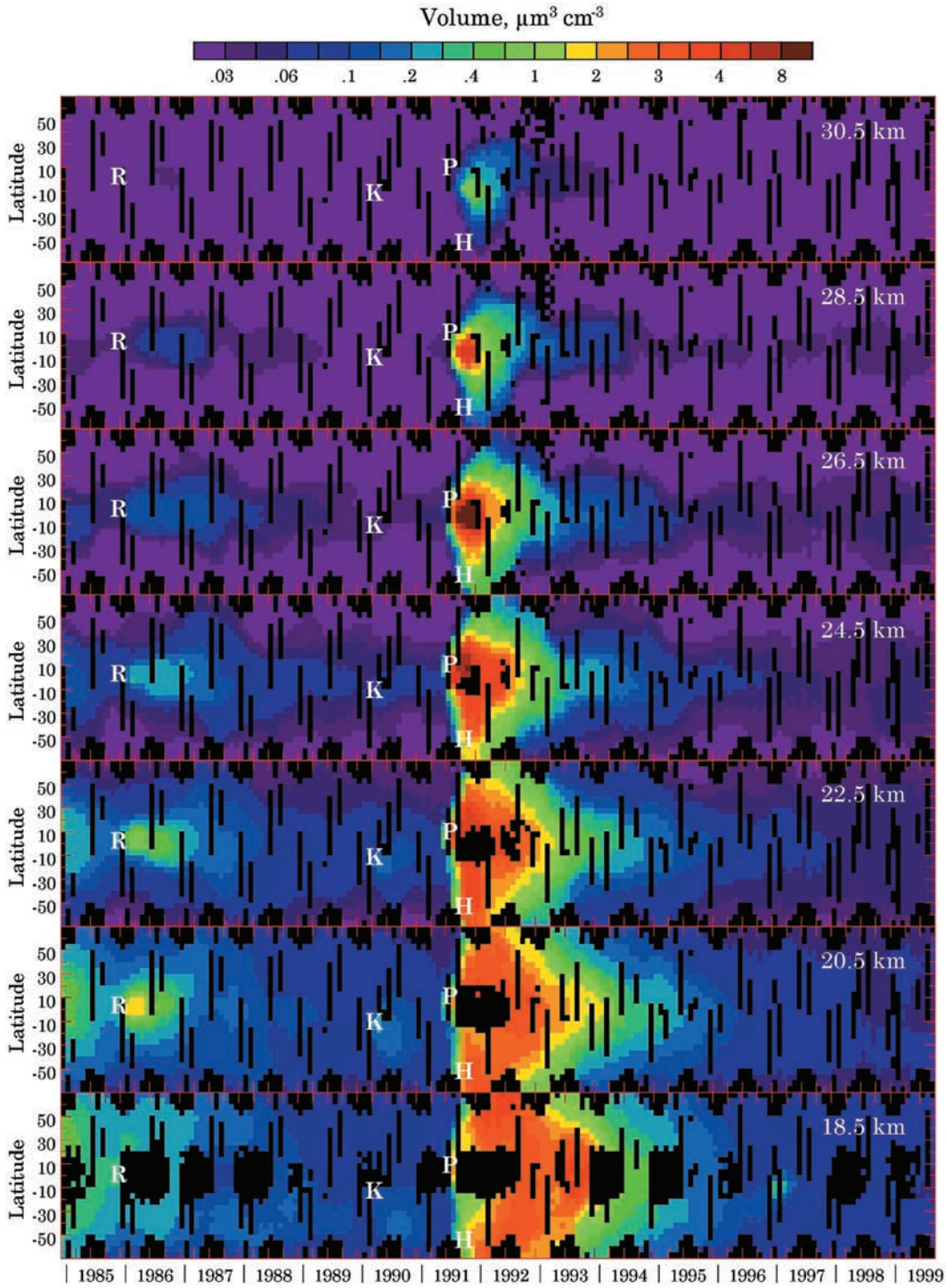

Figure 15. Latitude-time cross-sections of LUT-retrieved aerosol volume density V at 18.5, 20.5, 22.5, 24.5, 26.5, 28.5 and 30.5 km. The letters repeated in each frame mark the latitude and time of the Ruiz (R), Kelut (K), Pinatubo (P) and the Hudson (H) eruptions.

particle surface area as function of altitude above Laramie, Wyoming (41°N) using balloon-borne measurements of size distribution; (2) *Hitchman et al.* [1994], who compiled nearly a decade (1979–1981 and 1984–1990) of 1 μm extinction measurements from SAGE, SAGE II and SAM II extending from the tropopause to 35 km, between 80°S and 80°N. This data set was used to construct a decadal-average particle surface area climatology; (3) *Grainger et al.* [1995], who used relationships between effective radius, surface area and volume from balloon-borne measurements to estimate aerosol properties from measurements of the absorption coefficient at a single infrared wavelength. *Lambert et al.* [1997] applied this technique to a composite of CLAES and ISAMS data from September 1991 to April

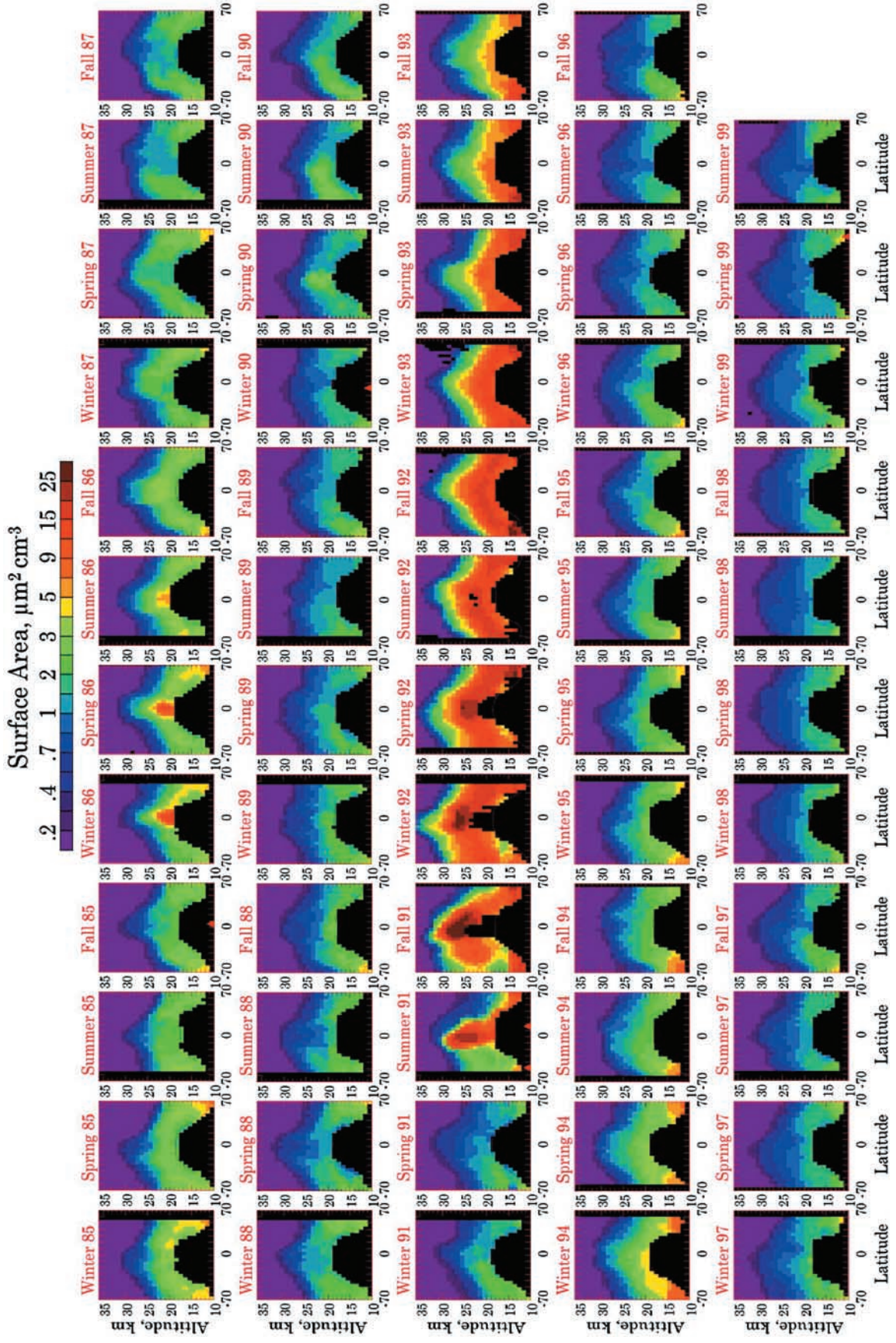

Figure 16. Seasonally averaged surface area *S* retrieved by the LUT, Winter (DJF) 1985 to Summer (JJA) 1999.

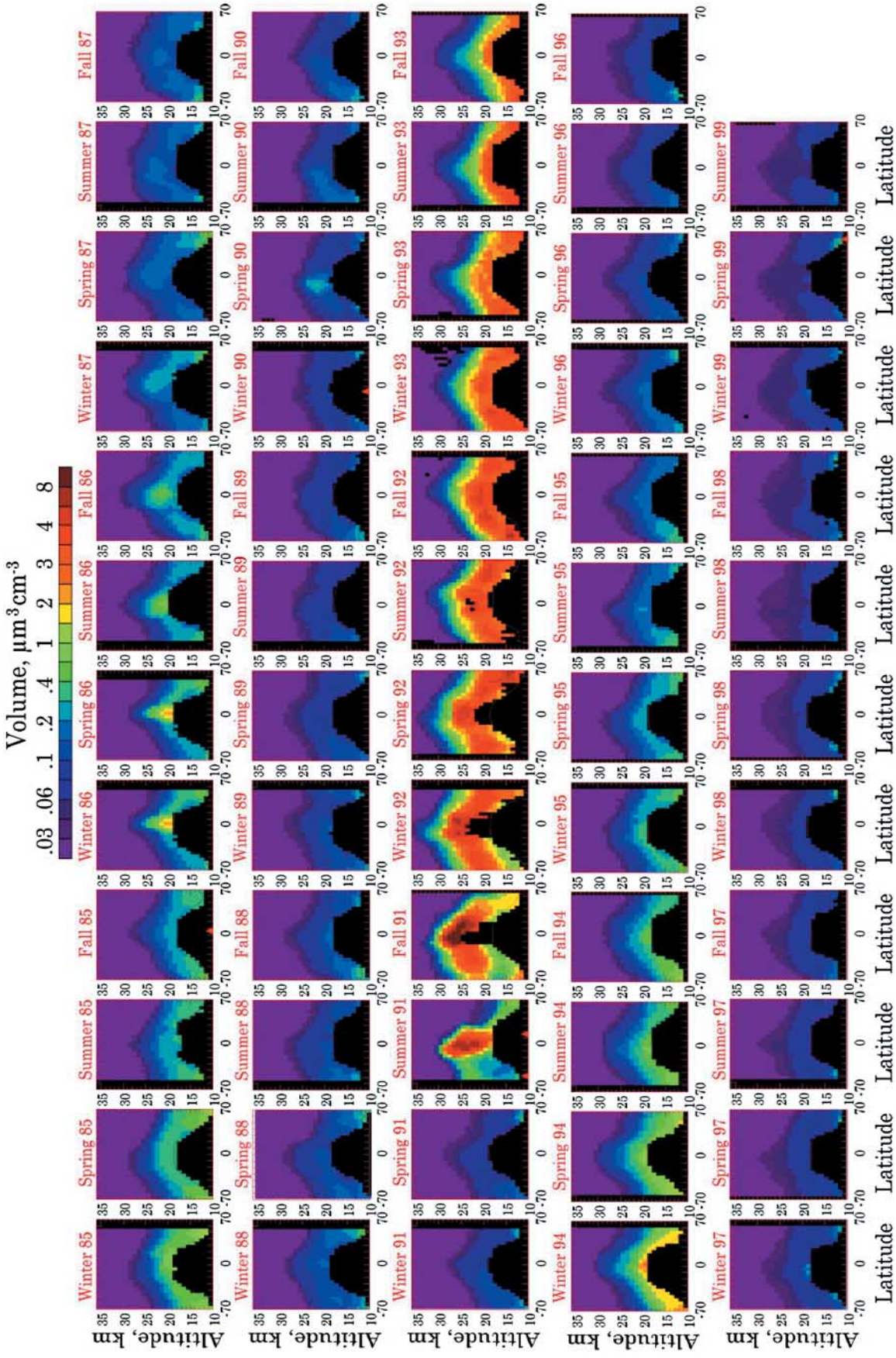

Figure 17. Seasonally averaged volume *V* retrieved by the LUT, Winter (DJF) 1985 to Summer (JJA) 1999.

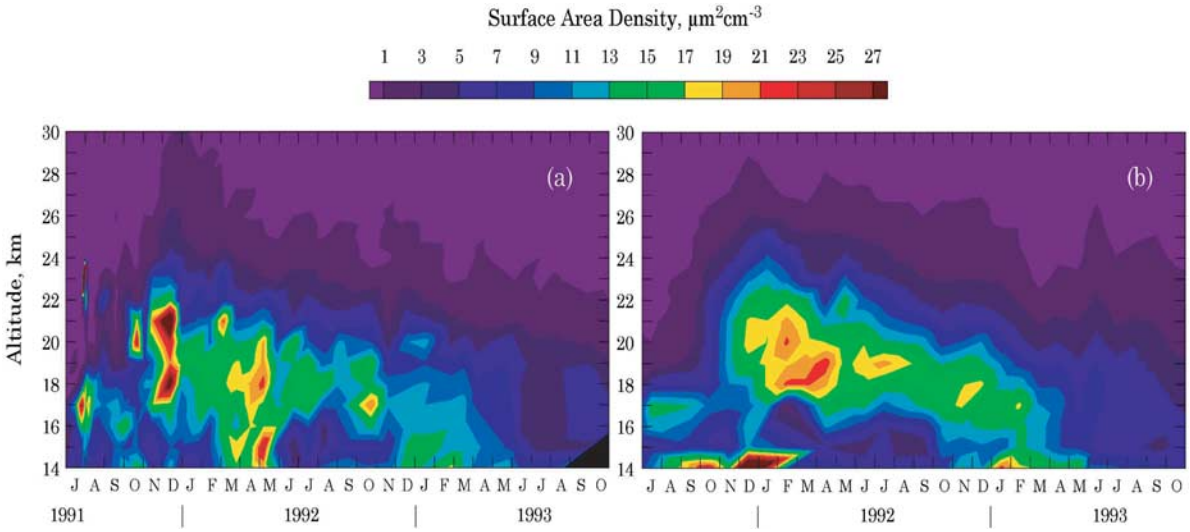

Figure 18. Altitude-time contours of aerosol surface area density *S*. (a) Values of *S* over Laramie, Wyoming (41°N) derived by *Deshler et al.* [1993] using lognormal fits to in situ size distributions. (b) LUT retrieved values of *S* in the latitude band 40° to 45°N.

1993 in order to construct zonal mean distributions of R_{eff}, *S*, and *V* from 80°S to 80°N; (4) *Kent et al.* [1995], who used ratios of SAGE II 0.525 μm to 1 μm extinctions to derive particle effective radius from 1984 to the Pinatubo eruption in six latitude bins from 60°N to 60°S; and (5) *Thomason et al.* [1997], who produced a 1984–1995 climatology of stratospheric aerosol surface area at 15.5, 20.5, 25.5 and 30.5 km using principal component analysis (PCA) with SAGE II data, and an extended (1979–1994) climatology at 20.5 km by combining SAGE II data with the single-wavelength measurements of SAM II and SAGE.

5.1. *Deshler et al.* [1993] Surface Area Climatology

[31] Vertical profiles of aerosol size distribution have been measured by *Deshler et al.* [1993] since July 1991 over Laramie, Wyoming using balloon-borne optical particle counters (OPC). Lognormal distributions are used to represent OPC measurements of integral number density. In an optimization scheme, distribution parameters are selected to minimize the difference between the analytical and measured number concentration for each size measurement [*Hofmann and Deshler*, 1991]. *Deshler et al.* [1993] used the distributions to construct a time history of particle surface area as function of altitude. Figure 18a shows a contour plot of the *Deshler et al.* [1993] results, which extend through 1992; also included are unpublished results for 1993 [T. Deshler, personal communication]. The *Deshler et al.* [1993] initial estimates of surface area, on the order of 1 $\mu m^2 cm^{-3}$ in the stratosphere, increased quickly after Pinatubo by a factor of 10 to 20 below 25 km. Observations over Laramie one month after the eruption show a narrow aerosol layer between 15 and 18 km, with occasional layers between 21 and 23 km [*Deshler et al.*, 1992]. On 30 July 1991 the upper layer exhibited a short-lived, intense maximum with surface area on the order of 84 $\mu m^2 cm^{-3}$. Vertical aerosol distribution was very structured and inhomogeneous for the first two months following Pinatubo [*Deshler et al.*, 1992]. From September to November 1991 the aerosol filled the stratosphere between the tropopause and 27 km but maintained a highly layered structure, indicating that vertical mixing was not complete. A second stratospheric maximum of greater that 27 μm^2 cm^{-3} occurred in December 1991 near 21 km, as seen in Figure 18a. *Deshler et al.* [1993] observed that during the first half of 1992, the surface area maximum remained relatively constant between 10 and 30 $\mu m^2 cm^{-3}$ from the tropopause to 25 km. The concentration of aerosols gradually declined after mid-1992, with the surface area peak occurring at progressively lower altitudes.

[32] For comparison, Figure 18b shows LUT retrievals of zonal mean surface area between 40° and 45°N. In general, the agreement is good, especially for altitudes above about 22 km and for times after mid-1992. Pre-Pinatubo surface areas retrieved by the LUT are also consistent with balloon-borne estimates of approximately 1 $\mu m^2 cm^{-3}$. Like the results of *Deshler et al.* [1993], LUT retrievals show an initial aerosol layer one month after the eruption of Pinatubo between 15 and 18 km. However, the short-lived, intense, upper aerosol layer near 21 to 23 km noted by Deshler et al. was not observed in LUT surface areas. Figure 18b shows the maximum surface area occurring in January 1992, one to two months after the in situ measured maximum over Laramie. In addition, LUT-estimated peak values are only on the order of 22 $\mu m^2 cm^{-3}$, which is at least 5 $\mu m^2 cm^{-3}$ less than the peak shown in Figure 18a. Finally, the altitude of the peak retrieved by the LUT tends to gradually decline after mid-1992, suggesting sedimentation and removal of the Pinatubo aerosol to the troposphere. This is consistent with the results published by *Deshler et al.* [1992].

[33] The discrepancies noted above may be due to the difference in observation location between the two estimates. That is, while the *Deshler et al.* [1993] results are determined at one latitude and longitude (41°N, 106°W), LUT retrievals are zonal averages and apply to a five degree latitude band (40° to 45°N). As mentioned above, values of aerosol surface area peak progressively later and have smaller maximum values at higher latitudes. Since Laramie lies near the equatorward edge of the latitude band used by

the LUT, the Deshler et al. surface area maximum should be greater and occur sooner than the LUT surface area maximum, as it does. It should be pointed out that there is some uncertainty in the Deshler et al. measured aerosol concentrations that impacts uncertainty in lognormal parameters and derived surface area. Results of Monte Carlo simulations performed by *Thomason et al.* [1997] suggest an average uncertainty of 10 to 20% and a maximum uncertainty of 30 to 40% in OPC surface area estimates.

5.2. *Hitchman et al.* [1994] Surface Area Climatology

[34] *Hitchman et al.* [1994] compiled nearly a decade (from February 1979 to November 1981 and from October 1984 to December 1990) of 1 μm extinction measurements from SAGE, SAGE II and SAM II extending from the tropopause to 35 km, and between 80°S and 80°N. This data set was used to construct a decadal-average particle surface area climatology. The conversion method used to calculate surface area from extinction measurements is based on lidar and optical particle counter measurements made by *Jäger and Hofmann* [1991] over Wyoming. Jäger and Hofmann calculated ratios of surface area-to-backscatter and extinction-to-backscatter averaged from 1980 to 1987 in three altitude bins (i.e., 15–20 km, 20–25 km and 25–30 km). Hitchman et al. then fit vertical profiles to the averaged ratios that were contemporaneous with satellite aerosol data during the periods 1980–1981 and 1985–1987. The resulting formula for converting observed aerosol extinction to surface area density gives values of S that increases linearly above the tropopause. It is given by:

$$S_{y,z}(\mu m^2 cm^{-3}) = \left[0.8\left(z - z_{trop}\right)/20 + 0.7\right] \times 10^4 \times \beta_{y,z}(km^{-1}) \quad (2)$$

Here, $S_{y,z}$ and β_{yz} are the aerosol surface area and extinction at 1 μm, respectively, at a given latitude, y, and altitude, z. The height of the tropopause, z_{trop}, also varies with latitude.

[35] Results of applying this formula to decadal-averaged 1 μm extinctions are shown in Figure 19a. Within 5 km of the tropopause, surface area estimates are approximately 3 $\mu m^2 cm^{-3}$ on the decadal average, and exceed 4 $\mu m^2 cm^{-3}$ in the tropics and north polar region. Figure 19b shows corresponding LUT-retrieved values of S averaged over 6 years, from December 1984 to December 1990. LUT retrievals are not calculated prior to December 1984, and so exclude the relatively low aerosol loading period from February 1979 to November 1981. Thus the six-year LUT average should be greater than the decadal average presented by *Hitchman et al.* [1994]. However, Figure 19 shows that this is not the case. The LUT estimates a smaller tropical peak of approximately 3 to 4 $\mu m^2 cm^{-3}$, and a midlatitude to high-latitude peak between 2 and 3 $\mu m^2 cm^{-3}$. The discrepancy may be due to the fact that ratios of surface area density-to-backscatter and extinction-to-backscatter measured by *Jäger and Hofmann* [1991] varied considerably over the observational period. This results in a relative uncertainty of approximately 50% in surface area density calculated by equation (2) [*Hitchman et al.*, 1994]. Furthermore, Jäger and Hofmann only use measurements obtained at one location, over Wyoming. Hitchman et al. state that the conversion contains a great deal of uncertainty due to the relative lack of knowledge of the global variation of aerosol size distribution and its evolution following an eruption.

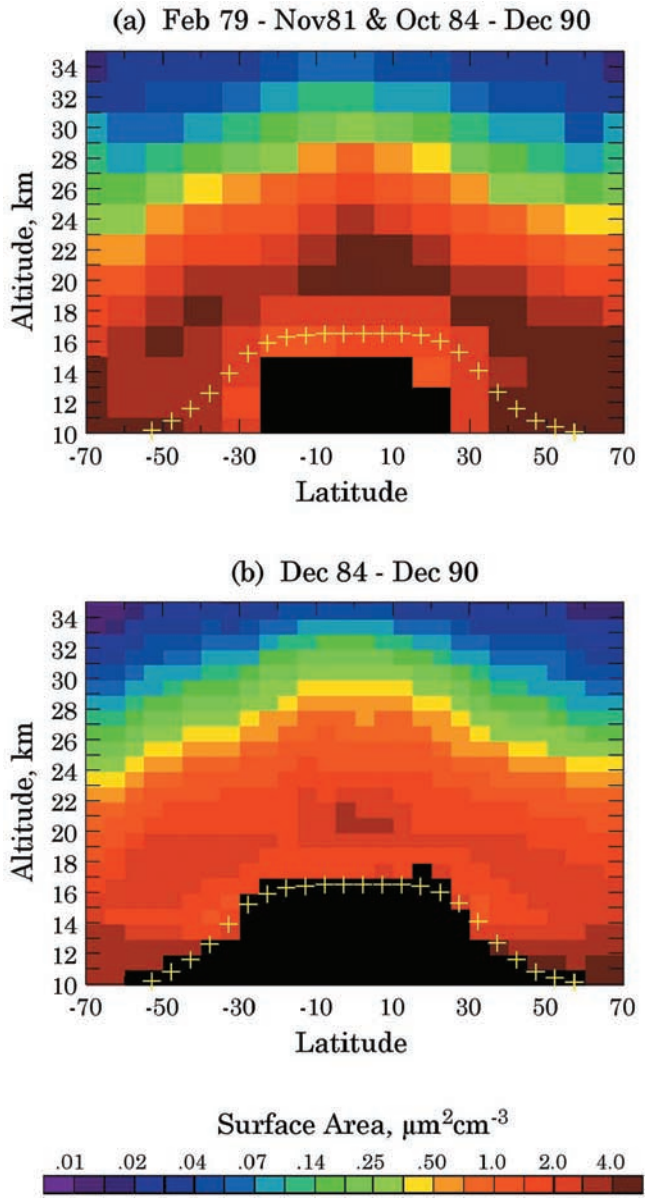

Figure 19. Altitude-latitude cross sections of near-decade averages of aerosol surface area density S. (a) Values of S from *Hitchman et al.* [1994] based on ~ 9.1 years (February 1979 to November 1981, and October 1984 to December 1990) of contemporaneous SAGE, SAGE II and SAM II extinction measurements. (b) LUT-retrieved values of S averaged over 6 years (December 1984 to December 1990). Crosses mark the tropopause height averaged from December 1984 to December 1990.

[36] Both estimates of surface area presented in Figure 19 exceed by an order of magnitude the values observed in 1979, which are often described as "background". *Hitchman et al.* [1994] suggest that minimum equilibrium aerosol values were not reached during the data record, and that the decadal average is distinctly volcanic in nature. This may also explain the differences noted in the two estimates of surface area. As discussed in paper 1, volcanic aerosols are often best

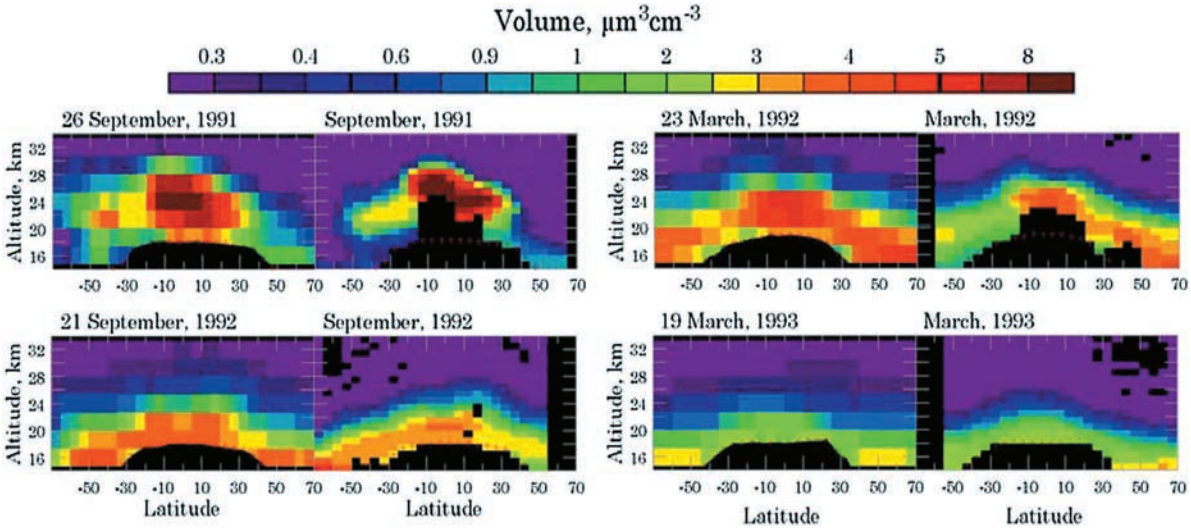

Figure 20. Altitude-latitude cross sections of aerosol volume V from September 1991 to March 1993. Values on the left in each column are estimates of V for a single day from *Lambert et al.* [1997] based on methods of *Grainger et al.* [1995], while values on the right are LUT retrievals of V for the indicated month. The plus symbols in each frame mark the tropopause plus 2 kilometers.

described as bimodal. Surface areas reported by *Jäger and Hofmann* [1991] were calculated from bimodal distributions. However, the LUT is based on a unimodal lognormal, and tends to underestimate retrievals of S during periods strongly influenced by volcanic eruptions (paper 1). LUT retrievals are not corrected for the assumption of unimodality prior to June 1991. This may bias low the retrievals of S shown in Figure 19b, particularly below 22 km.

[37] Nevertheless, there is good quantitative agreement between the two estimates above and below the peak at all latitudes. Qualitatively the two estimates are quite similar in that both exhibit peaks between 19 and 23 km in the tropics, with slightly larger values at northern high latitudes than at southern high latitudes. In both cases, the peak slopes downward with latitude, but is located at nearly a constant altitude above the tropopause.

5.3. *Lambert et al.* [1997] Aerosol Climatology

[38] *Grainger et al.* [1995] used relationships between effective radius, surface area and volume from balloon-borne measurements to estimate aerosol properties from measurements of the absorption coefficient at a single infrared wavelength. *Lambert et al.* [1997] applied the technique to a composite of CLAES and ISAMS data near 12 μm. The ISAMS instrument measured thermal emissions from the Earth's limb in several spectral regions [*Taylor et al.*, 1993] from September 1991 to July 1992 [*Rodgers et al.*, 1996]. Lambert et al. constructed zonal mean climatologies of aerosol volume, surface area and effective radius from September 1991 to April 1993 and from 80°S to 80°N.

[39] Aerosol volume is the fundamental parameter derived from the long wavelength extinction measurements of ISAMS and from which surface area and effective radius were deduced. The left frames in Figure 20 show the *Lambert et al.* [1997] estimates of V for the time indicated at the top of each frame. Lambert et al. calculated percent errors in volume estimates to be less than 20% except near the tropopause and at high altitudes, where the measurement uncertainties are larger. For comparison, LUT retrievals of zonal/monthly mean aerosol volume during corresponding months are shown in the right frames. SAGE II saturation in the lower tropical stratosphere is evident until about May 1992. Both methods estimate a volume maximum in the tropics greater than 8 $\mu m^3 cm^{-3}$ between 23 and 26 km in September 1991, with no evidence of increase thereafter. Both methods are also consistent in showing that by March 1993, maximum volume densities of 1 to 3 $\mu m^3 cm^{-3}$ occurred within 3 km of the tropopause, with slightly larger values at high latitudes. In general, there is good qualitative agreement in the shape of the aerosol cloud and in the gradual decline of the volume peak altitude with time. However, above the aerosol layer peak the Lambert et al. volume estimates tend to be slightly greater than those values retrieved by the LUT.

[40] The zonal mean surface area distributions show that for most times and locations the *Lambert et al.* [1997] values of S are larger than those retrieved by the LUT, particularly in the densest part of the aerosol cloud. Lambert et al. estimates a broad maximum in S between 20°N and 15°S of nearly 50 $\mu m^2 cm^{-2}$ from 23 to 26 km in September 1991. For the same time and location, the LUT retrieves smaller values of surface area density on the order of 24 $\mu m^2 cm^{-3}$. By March 1993, the Lambert et al. values of S decreased to approximately 10 $\mu m^2 cm^{-3}$, while LUT retrievals of S decreased to about 6 $\mu m^2 cm^{-3}$ in the stated latitude and altitude range. Further comparisons with the Lambert et al. surface area estimates are presented in section 5.5.

[41] Analogous comparisons were made for R_{eff} estimated by *Lambert et al.* [1997] and retrieved by the LUT. Lambert et al. obtain an effective radius in the tropics that decays monotonically from a peak of approximately 0.65 μm in September 1991 to 0.4 μm in March 1993. Values of R_{eff} retrieved by the LUT do not decrease monotonically with time, but exhibit latitude- and altitude-dependent peaks that occur after September 1991. The Lambert et al. peak values of R_{eff} decay much more quickly than do the LUT-retrieved

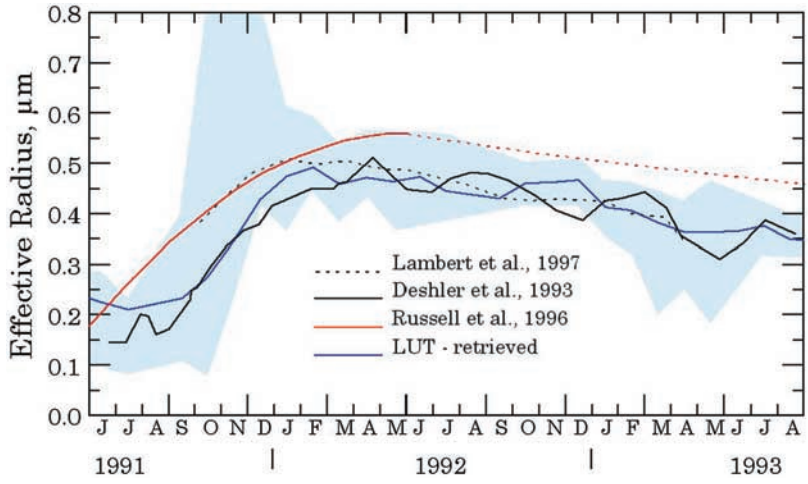

Figure 21. Time series of aerosol effective radius. The dashed black line is from *Lambert et al.* [1997] at 41°N and 18.7 km; the solid black line is from *Deshler et al.* [1993] at 41°N and 18.7 km using balloon-borne OPC measurements; the solid and dashed red line is from *Russell et al.* [1996] using an empirical fit to an ensemble of measurements; and the solid blue line and shading are the LUT-retrieved value and uncertainty in the 40°–45°N latitude band at 18.5 km.

peak values. By March 1993, the LUT values of R_{eff} remain near 0.5 μm in a layer just above the tropopause. Finally, the Lambert et al. estimates of R_{eff} tend to be larger than the LUT retrievals above the bulk of the aerosol cloud and smaller in the densest part of the cloud down to the tropopause.

[42] The discrepancies noted in aerosol retrievals at high altitudes may be due to ISAMS failing to resolve the sharp decrease in extinction above the aerosol layer. Above the aerosol peak ISAMS extinction estimates are biased high [*Lambert et al.*, 1996]. *Grainger et al.* [1995] report that above about 22 km, the large bias in ISAMS measurements results in large uncertainties in aerosol parameters retrieved using the above technique. A systematic error may also be introduced when applying the Grainger et al. technique to global extinction measurements because this technique was based on size distributions obtained from balloon measurements made at high northern latitudes.

[43] In general, the best agreement is between aerosol volume density estimates, the variable most directly related to ISAMS and CLAES longwave extinction measurements. The technique is based on a single time- and space-independent relationship between surface area and volume, and therefore estimates of V, S and R_{eff} will always vary together. As a result, the Lambert et al. estimates of V, S and R_{eff} exhibit similar decay rates. For example, the decay rate of R_{eff} determined by *Lambert et al.* [1997], while much quicker than the decay rate of R_{eff} retrieved by the LUT, is similar to the Lambert et al. surface area and volume decay rates. Graphical comparisons of R_{eff}, S and V from LUT retrievals and from ISAMS are presented by *Bauman* [2000].

[44] Figure 21 shows a time series of aerosol effective radius deduced from a variety of techniques. The dashed black line is from *Lambert et al.* [1997] at 41°N and 18.7 km. The solid black line is from *Deshler et al.* [1993] at 41°N and 18.7 km using balloon-borne OPC measurements. The solid and dashed red line is from *Russell et al.* [1996] using empirical fits to an ensemble of measurements. The solid blue line and shading are the LUT-retrieved value and uncertainty in R_{eff} in the 40°–45°N latitude band at 18.5 km. In general, all values agree to within the LUT error bars, with slightly larger values of R_{eff} outside this range given by Russell et al. after mid-1992. As noted in the discussion of Figure 1 above, upper error bars on LUT-retrieved of R_{eff} are unbounded from the first month following Pinatubo until January 1992. This results from the spectrally flat shape of extinction spectra at SAGE II wavelengths, which by themselves give no upper limit on R_{eff}. Addition of the CLAES longwave extinction measurements in January 1992 greatly reduces the upper limit on the LUT-retrieved R_{eff} values.

5.4. *Kent et al.* [1995] Effective Radius Climatology

[45] *Kent et al.* [1995] used ratios of SAGE II 0.525 μm to 1.02 μm extinctions to derive particle effective radius from October 1984 to May 1991 in six latitude bands from 60°N to 60°S. Their method is based on the fact that the extinction ratio β(.525 μm)/β(1.02 μm) depends on the aerosol size distribution, with larger values of the ratio corresponding to smaller particles. They assume that stratospheric aerosols are spherical droplets of 75% H_2SO_4 whose distribution can be modeled with a unimodal lognormal. This approach is similar to the LUT in that it uses Mie theory to precompute the extinction ratio β(.525 μm)/β(1.02 μm). However, the Kent et al. approach differs from the LUT in the following ways: (1) it only uses extinction measurements at two SAGE II wavelengths; (2) it does not use uncertainty in extinction to determine error bars on retrievals of R_{eff}; and (3) it uses a fixed distribution width $\sigma_g = 1.7$, leaving only one free parameter, R_{eff}. Kent et al. assumes that the observed extinction is due primarily to particles with radii between 0.08 and 0.6 μm. This assumption is necessary since, as pointed out by *Wang et al.* [1989] and *Thomason* [1991], SAGE II extinction measurements give little information about particles smaller than about

0.1 μm and little size discrimination for particles larger than 0.8 μm. If appreciable numbers of particles with radii outside of these limits are present, radius information will be ambiguous since the extinction ratio β(.525 μm)/β(1.02 μm) is effectively a constant function of radius outside this range. The authors compare measured extinction ratios with precomputed ratios presented as a function of particle size to determine a single value of R_{eff} consistent with SAGE II 0.525 μm and 1.02 μm measurements.

[46] Using the above approach, *Kent et al.* [1995] estimate that R_{eff} varies in the tropical stratosphere from peak volcanic values on the order of 0.5 μm just above the tropopause in 1984 to 0.15 μm at the same altitude in 1989. We generated altitude-time cross sections of LUT-retrieved aerosol effective radius for the same times and locations as those published by Kent et al. LUT results yield peak values of R_{eff} in the tropics exceeding 0.38 μm just above the tropopause in December 1984 and early 1985, and declining to about 0.2 μm in 1989 at the same altitude. The El Chichón cloud is supplemented by aerosol from the eruption of Ruiz in November 1985 at 5°N. Values of R_{eff} peak in the stratosphere following Ruiz at about 0.35 μm in late 1986 to early 1987 at 20 km from the equator to 20°N. Increases in particle size following the eruption of Kelut in February 1990 were found southward of 20°S in the stratosphere. Six months after the eruption of Kelut, R_{eff} peaked at approximately 0.35 μm in the lower stratosphere from 20° to 40°S.

[47] Table 2 compare values of R_{eff} published by *Kent et al.* [1995] with corresponding values retrieved by the LUT at various times within six latitude bands. Also shown are estimates of R_{eff} derived from balloon-borne infrared polarimeter measurements of *Brogniez and Lenoble* [1988]; from balloon-borne optical particle counter measurements of *Hofmann* [1990] and *Deshler et al.* [1993]; and from passive cavity aerosol spectrometer measurements of *Wilson et al.* [1993]. Estimates of R_{eff} from Kent et al. are approximately 17% smaller than those values retrieved by the LUT within the above six latitude bands. Conversely, LUT retrievals are about 5% smaller than the average estimate of R_{eff} from *Brogniez and Lenoble* [1988], *Hofmann* [1990], *Deshler et al.* [1993] and *Wilson et al.* [1993]. The discrepancy noted between estimates from Kent et al. and those from the LUT is likely due to the fact that the LUT allows the distribution width to vary over a wide range of values and makes use all SAGE II extinction measurements.

Table 2. Stratospheric Aerosol Effective Radius Intercomparisons, 1984–1991[a]

Time	Latitude	Altitude, km	Effective Radius, μm	Source
Dec 1984	20°N–40°N	19.5	0.3–0.35	*Kent et al.* [1995]
Dec 1984	20°N–40°N	19.5	0.35	LUT
Dec 1984	Equator–20°N	18.5	0.45–0.5	*Kent et al.* [1995]
Dec 1984	Equator–20°N	18.5	0.54	LUT
Oct 1985	43°N	15	0.28	*Kent et al.* [1995]
Oct 1985	43°N	15	0.36	*Brogniez and Lenoble* [1988]
Oct 1985	40°N–45°N	15.5	0.37	LUT
Oct 1985	43°N	20	0.23	*Kent et al.* [1995]
Oct 1985	43°N	20	0.27	*Brogniez and Lenoble* [1988]
Oct 1985	40°N–45°N	20.5	0.27	LUT
Oct 1985	43°N	25	0.18	*Kent et al.* [1995]
Oct 1985	43°N	25	0.31	*Brogniez and Lenoble* [1988]
Oct 1985	40°N–45°N	25.5	0.18	LUT
Jan 1986	20°N–40°N	19.5	0.2–0.25	*Kent et al.* [1995]
Jan 1986	20°N–40°N	19.5	0.29	LUT
Jan 1986	40°S–20°S	17.5	0.25–0.3	*Kent et al.* [1995]
Jan 1986	40°S–20°S	17.5	0.29	LUT
Jan 1987	20°S–Equator	23.5	0.2–0.25	*Kent et al.* [1995]
Jan 1987	20°S–Equator	23.5	0.32	LUT
May 1987	Equator–20°N	19.5	0.3–0.35	*Kent et al.* [1995]
May 1987	Equator–20°N	19.5	0.33	LUT
Oct 1987	40°N–60°N	16.5	0.2–0.25	*Kent et al.* [1995]
Oct 1987	40°N–60°N	16.5	0.33	LUT
Nov 1987	20°S–Equator	19.5	0.3–0.35	*Kent et al.* [1995]
Nov 1987	20°S–Equator	19.5	0.32	LUT
May 1988	60°S–40°S	15.5	0.2–0.25	*Kent et al.* [1995]
May 1988	60°S–40°S	15.5	0.36	LUT
Dec 1988	37°N	19	0.14	*Kent et al.* [1995]
Dec 1988	37°N	19	0.25	*Wilson et al.* [1993]
Dec 1988	35°N–40°N	19.5	0.24	LUT
1989 average	41°N	18–22	0.13	*Kent et al.* [1995]
1989 average	41°N	18–22	0.26	*Hofmann* [1990]
1989 average	40°N–45°N	18.5–22.5	0.25	LUT
Jan 1990	40°N–60°N	23.5	0.15–0.2	*Kent et al.* [1995]
Jan 1990	40°N–60°N	23.5	0.21	LUT
June 1990	60°S–40°S	15.5	0.25–0.3	*Kent et al.* [1995]
June 1990	60°S–40°S	15.5	0.35	LUT
Dec 1990	40°S–20°S	23.5	0.15–0.2	*Kent et al.* [1995]
Dec 1990	40°S–20°S	23.5	0.21	LUT
Spring 1991	41°N	17–21	0.14	*Kent et al.* [1995]
Spring 1991	41°N	17–21	0.11–0.13	*Deshler et al.* [1993]
Spring 1991	40°N–45°N	17.5–21.5	0.24	LUT

[a]LUT retrievals of R_{eff} at various times and locations are compared with estimates from *Brogniez and Lenoble* [1988], *Hofmann* [1990], *Deshler et al.* [1993], *Wilson et al.* [1993], and *Kent et al.* [1995].

5.5. *Thomason et al.* [1997] Surface Area Climatology

[48] *Thomason et al.* [1997] produced a 1984 to 1995 climatology of stratospheric aerosol surface area at 15.5, 20.5, 25.5 and 30.5 km by applying principal component analysis (PCA) to SAGE II data. They also developed an extended (1979 to 1994) climatology at 20.5 km by combining SAGE II data with single-wavelength measurements from SAM II and SAGE. Both climatologies assume a constant aerosol composition of 75% H_2SO_4 and 25% H_2O by weight.

[49] The *Thomason et al.* [1997] results of applying PCA to SAGE II data are shown in Figures 22 and 23. Figure 22 presents time series of aerosol surface area near 15 km (top frame), 20 km (middle frame), and 25 km (bottom frame) from 15 June 1991 to 5 January 1995 (0 to 1300 days after the eruption of Pinatubo). Values of S are calculated by *Thomason et al.* [1997] using PCA applied to SAGE II data (black dots and error bars), and using particle size measurements from the University of Wyoming optical particle counters (OPC) (shading). PCA estimates are monthly zonal means ±1 standard deviation for the 35° to 45°N latitude band between 0.5 km above and below the altitude indicated in the upper left of each frame. OPC estimates reflect a range of surface area values calculated for each near-monthly balloon ascent over Laramie (41°N) in the altitude band 1 km above and below the indicated altitude. Also shown are values of S determined by *Lambert et al.* [1997] (compare section 5.3) (green crosses), and by applying the linear minimizing error (LME) technique of *Yue* [1999] to SAGE

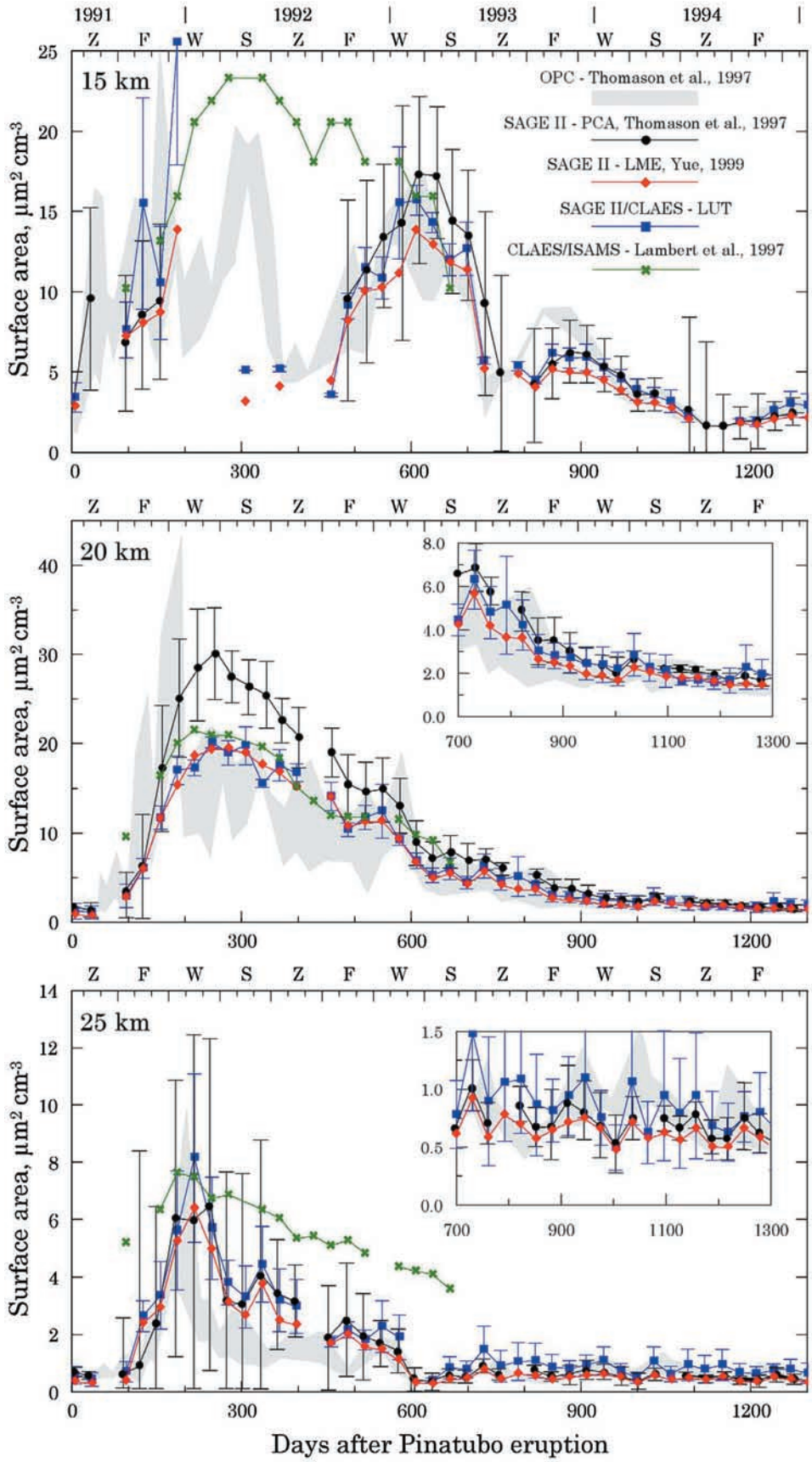
1991
1992
1993
1994
Z F W S Z F W S Z F W S Z F
15 km
20 km
25 km
OPC - Thomason et al., 1997
SAGE II - PCA, Thomason et al., 1997
SAGE II - LME, Yue, 1999
SAGE II/CLAES - LUT
CLAES/ISAMS - Lambert et al., 1997
Surface area, μm² cm⁻³
Days after Pinatubo eruption

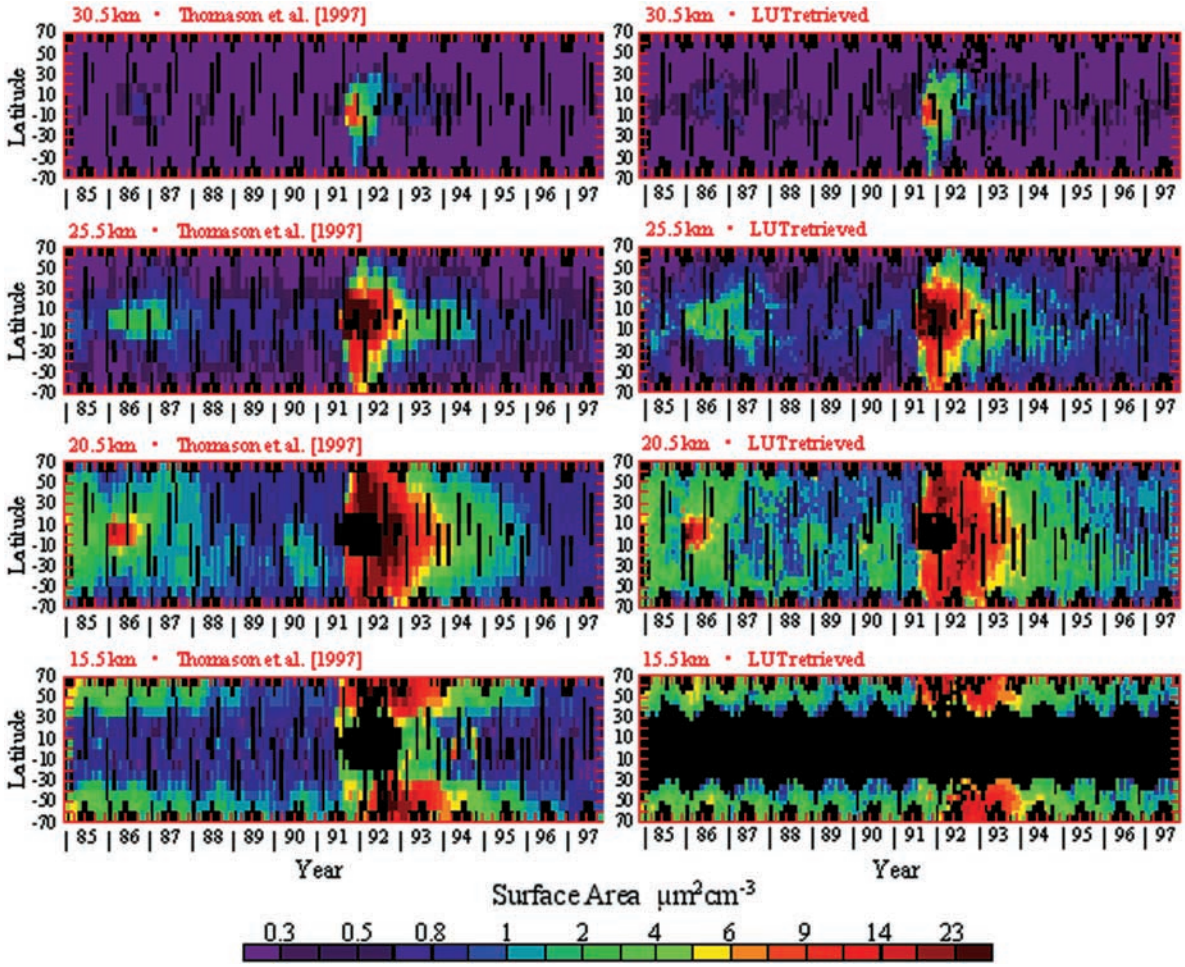

Figure 23. Latitude-time cross sections of aerosol surface area *S* at 30.5, 25.5, 20.5 and 15.5 km. Left frames: Values of *S* from *Thomason et al.* [1997] based on principal component analysis (PCA). Right frames: LUT retrieved values of *S*.

II data (red diamonds). (The LME is not a climatology but a technique for obtaining a size distribution from SAGE extinction measurements.) LUT retrievals are also shown (blue squares and error bars). The LME and LUT estimates are presented for the 40° to 45°N latitude band, between 0.5 km above and below the indicated altitude. LUT retrievals are monthly zonal means ±1 standard deviation. Estimates by Lambert et al. are presented for the 40° to 45°N latitude band at 16 ± 1.33 km, 20 ± 2.67 km, and 25 ± 2.67 km, respectively. Inset graphs show enlargements of respective results from day 700 to 1300. Seasonal fluctuations are evident in all retrievals, particularly near 15 km. In general, estimates of *S* based on SAGE II data (i.e., values from the PCA, LME and LUT techniques) agree quite well with OPC estimates during the initial posteruption aerosol enhancement (day 0–200). After approximately Fall 1992 (∼day 500), during the gradual aerosol decline, all values agree within mutual error bars. An exception is retrievals from Lambert et al. at 25 km, which are 5 standard deviations or more above the maximum OPC values. During the period from December 1991 to Fall 1992 (day 200 to 500), there is less consistency among the various retrieval techniques. For example, at 20 km, zonal mean PCA estimates are approximately 2 standard deviations above the maximum OPC values. All other retrieval methods give similar results at this altitude, with peak surface areas reaching 21 $\mu m^2 cm^{-3}$

Figure 22. (opposite) Time series of *S* near 15 km (top frame), 20 km (middle frame), and 25 km (bottom frame) from 15 June 1991 to 5 January 1995. Values are calculated by *Thomason et al.* [1997] using PCA applied to SAGE II data (black dots and error bars), and using particle size measurements from the UW-OPC (shading). Also shown are values determined by *Lambert et al.* [1997] (green crosses), and by applying the LME technique [*Yue*, 1999] to SAGE II data (red diamonds). LUT retrievals are the blue squares and error bars. PCA estimates are monthly zonal means ±1σ for 35° to 45°N between ±0.5 km relative to the altitude indicated in the upper left of each frame. OPC measurements are for 41°N between ±1 km relative to the indicated altitude. LME and LUT estimates are for 40° to 45°N between ±0.5 km relative to the indicated altitude. LUT retrievals are monthly zonal means ±1σ. Estimates by Lambert et al. are for 40 to 45°N, at 16 ± 1.33 km, 20 ± 2.67 km, and 25 ± 2.67 km, respectively.

during February 1992 (~day 250). At 25 km, estimates based on SAGE II data exceed OPC values, but agree remarkably well with each other. The greatest discrepancy during this period is with the Lambert et al. surface area estimates at 15 and 25 km, which are 2 to 10 standard deviations above OPC values. Gaps in the PCA, LME and LUT estimates near 15 km during this period are due to SAGE II saturation. The observed differences between OPC estimates and all other estimates may be due to zonal variability since the PCA, LME, LUT and the Lambert et al. values are zonal averages, while OPC measurements are obtained over Laramie. On the other hand, the discrepancies noted between SAGE II-based estimates are due to differences in retrieval techniques.

[50] Figure 23 compares values of surface area from *Thomason et al.* [1997] using PCA with LUT retrievals of S at 30.5, 25.5, 20.5, and 15.5 km as a function of latitude and time. The Thomason et al. values are binned monthly (with a 2-month sampling window) and every 10° latitude. LUT retrievals in the tropics are not shown at 15.5 km as this is below the tropopause plus 2 kilometers. In general, both estimates agree well in showing the shape of the aerosol cloud. The Thomason et al. estimates are slightly larger than LUT retrievals when values of S are greater than approximately 20 $\mu m^3 cm^{-3}$, and smaller then LUT retrievals when values of S are less than approximately 6 $\mu m^2 cm^{-3}$. Thus Thomason et al. values of surface area are less than LUT retrievals of S during near-background periods (e.g., 1989 to mid-1991, and after 1996), and greater than LUT retrievals in the peak of the Pinatubo plume. This is consistent with Figure 22.

6. Conclusions

[51] Aerosol parameters retrieved by applying the LUT algorithm to the SAGE II and CLAES data sets are presented as zonal averages in 1 month × 5° latitude × 1 km altitude sampling bins. The stratospheric aerosol climatology ranges from 10 to 40 km in altitude, includes latitudes between 70°N to 70°S, and spans nearly 15 years from December 1984 to August 1999. This period encompasses the El Chichón recovery period, a period of several small volcanic eruptions, a two to three year low-aerosol-loading period beginning in 1989, the June 1991 eruption of Mount Pinatubo, three to four years of post-Pinatubo aerosol dissipation, and approximately 3 years of record low aerosol mass loading from 1996 to 1999. Some of the more interesting features revealed in the climatology include the following: (1) Retrievals of R_{eff}, S and V show notable increases after most major volcanic eruptions. Exceptions include the effects of Kelut, which are not apparent in retrievals of R_{eff} at any altitude above 18 km or in retrievals of S and V above 26 km. (2) Several months prior to the eruption of Pinatubo, SAGE II extinction spectra decreased monotonically with wavelength, and corresponding retrievals of R_{eff} were at near-background values of ~0.22 μm. (3) Immediately after Pinatubo, the peak in measured SAGE II extinction spectra shifted toward longer wavelengths, from 0.385 μm prior to Pinatubo to 0.525 μm in July 1991. Corresponding retrievals of R_{eff} increased to 0.5 μm or larger. Extinction spectra at SAGE II wavelengths (i.e., 0.385–1.02 μm) became flat within error bars, and hence upper error bars on retrieved R_{eff} were unbounded from this time until January 1992, when CLAES infrared extinction measurements became available. (4) The SAGE II extinction spectra remained spectrally flat within measurement uncertainty for nearly 2 1/2 years after Pinatubo, until January 1993, and retrievals of R_{eff} remained above 0.5 μm. (5) Peaks in retrieved R_{eff} lagged peaks in optical depth (at all wavelengths) and in retrieved surface area and volume density. (6) A declining trend in weighted-mean values of σ_g was noted from December 1984 to just before the Pinatubo eruption, followed by a sharp increase in σ_g after June 1991. Immediate postvolcanic increases in σ_g indicate broader size distributions and are consistent with sudden increases in both small and large particle sizes. (7) The sharpest increases in σ_g occur in the peak of the Pinatubo plume, between 20 and 26 km. At altitudes above 30 km, no significant variation was noted in the mean distribution width over time. (8) After the eruption of Pinatubo, column values of R_{eff}, S and V peak progressively later at higher latitudes. The time delay in peaking at midlatitudes to high latitudes is likely due to poleward transport of larger aerosol particles from the tropical reservoir rather than in situ growth by condensation and coagulation. (9) Values of R_{eff} evolved differently with respect to altitude after the eruptions of Ruiz and Pinatubo. Following both eruptions, the duration of the R_{eff} peak was shorter at progressively higher altitudes. However, unlike Pinatubo, values of R_{eff} peaked later in time at successively higher altitudes following Ruiz. It is unclear why values of R_{eff} peaked so late at high altitudes following Ruiz. (10) After approximately January 1993, the visible to near-IR extinction spectra in the 15–20°N latitude band began to peak at progressively shorter wavelengths, indicating the start of a return toward pre-Pinatubo spectral shapes. Concurrently, estimates of R_{eff} began to decay slowly toward pre-eruption values. (11) Six months after the eruptions of Ruiz and Pinatubo, values of σ_g declined sharply in the tropics, presumably due to rapid growth of smaller particles and preferential sedimentation-removal of larger particles. (12) Retrieved R_{eff} and σ_g took nearly five years, until mid-1996, to return to pre-Pinatubo values. Slightly shorter recovery times were obtained for S and V. (13) During near-background periods, size distribution widths gradually narrow with time at all latitudes and altitudes. This may be related to smaller particles growing and larger particles settling out. (14) During the low-aerosol-loading period, 1998 and 1999, size distributions narrow in going from the tropical core to higher latitudes at altitudes between approximately 20 and 22 km. (15) At the end of the data record, in January 1999, the stratospheric aerosol reached record low values of both measured optical and retrieved physical parameters. (16) There was no strong indication of an R_{eff} peak above the tropical tropopause in the absence of volcanic aerosol. (17) Seasonal variations in column S and V were observed at high latitudes (with high values occurring in Winter), but were less obvious in retrievals of R_{eff}. Seasonal extremes in S and V are most pronounced in the northern hemisphere. (18) Latitudinal banding was often noted in retrievals of R_{eff} during most near-background periods in a layer just above the tropopause, with high values occurring in the tropics and at high latitudes.

[52] Although accurate characterization of aerosols in the form of detailed size distribution information cannot be

obtained by the LUT algorithm (or through measurements of extinction in general), integrated properties such as particle effective radius, surface area density and volume density have been retrieved using the methods developed in this investigation.

[53] Several large data sets of the stratospheric aerosol layer have been produced previously by a variety of space-borne, air-borne, and ground-based sensors and samplers. Several of these climatologies, and the methods used to produce them, are reviewed in detail and compared with retrievals of aerosol properties obtained with our look-up table technique. With few exceptions, LUT retrievals agree well with most previously published climatologies. The following summarizes the findings of these comparisons:

[54] 1. *Deshler et al.* [1993] determined a time history of particle surface area as a function of altitude above Laramie, Wyoming (41°N) using balloon-borne measurements of size distribution. LUT-retrieved values are similar, especially for altitudes above 22 km and for times prior to Pinatubo and after mid-1992. The slight discrepancy noted in the magnitude and time of the Pinatubo plume peak is due to differences in observation location and the fact that the SAGE II results are averages whereas the OPC data are ''snapshots''.

[55] 2. *Hitchman et al.* [1994] compiled nearly a decade (1979–1981 and 1984–1990) of 1 μm extinction measurements from SAGE, SAGE II and SAM II extending from the tropopause to 35 km, between 80°S and 80°N. This data set was used to construct a decadal-average particle surface area climatology. There is quantitative agreement with LUT retrievals of surface area above and below the aerosol peak at all latitudes, and qualitative agreement in the shape of the aerosol cloud. However, LUT estimates of S are slightly smaller in the tropical peak than are values by Hitchman et al.

[56] 3. *Grainger et al.* [1995] used relationships between effective radius, surface area and volume from balloon-borne measurements to derive constraints for estimating aerosol properties from measurements of the absorption coefficient at a single infrared wavelength. *Lambert et al.* [1997] applied this technique to a composite of CLAES and ISAMS data from September 1991 to April 1993 in order to construct zonal mean distributions of R_{eff}, S, and V from 80°S to 80°N. In general, the best agreement is between aerosol volume density estimates. The large discrepancies noted between estimates of S and R_{eff} result because the Grainger et al. technique is based on a single time- and space-independent relationship between surface area and volume, and therefore estimates of V, S and R_{eff} always vary together.

[57] 4. *Kent et al.* [1995] used ratios of SAGE II 0.525 μm to 1 μm extinctions to derive particle effective radius from 1984 to the Pinatubo eruption in six latitude bins from 60°N to 60°S. Estimates of R_{eff} from Kent et al. are approximately 17% smaller than those values retrieved by the LUT. Although this difference is within the uncertainties of the LUT method, the systematic discrepancy is likely due to the LUT allowing the distribution width to vary over a wide range of values and using all SAGE II wavelengths.

[58] 5. *Thomason et al.* [1997] produced a 1984–1995 climatology of stratospheric aerosol surface area at 15.5, 20.5, 25.5 and 30.5 km using Principal Component Analysis (PCA) with SAGE II data. In general, both estimates of surface area agree well in showing the shape of the Pinatubo aerosol cloud. The Thomason et al. estimates are slightly larger than LUT retrievals when values of S are greater than approximately 20 $\mu m^2 cm^{-3}$, and are smaller then LUT retrievals when values of S are less than approximately 6 $\mu m^2 cm^{-3}$. Thus Thomason et al. values of surface area are less than LUT retrievals of S during near-background periods, and greater than LUT retrievals in the peak of the Pinatubo plume. The smaller LUT-derived surface areas during the Pinatubo peak result from the constraint provided by the CLAES 12.82 μm extinction measurements. During the peak of the Pinatubo plume near 20 km, PCA estimates are also two standard deviations above maximum S estimates by *Lambert et al.* [1997] based on CLAES/ISAMS data, and by *Thomason et al.* [1997] using particle size measurements from the University of Wyoming optical particle counter.

[59] On the basis of our comparisons, we suggest that the LUT technique is an accurate method for generating a global aerosol climatology from satellite extinction measurements under the variety of stratospheric conditions that existed from December 1984 to August 1999. The LUT climatology has advantages over some previously published climatologies for several reasons, including: (1) The15-year period included in the LUT data set extends beyond the periods of many previously produced data sets; (2) The LUT retrieval technique that produced this aerosol data set uses a composite of two independent global satellite extinction data sets from SAGE II and CLAES. This is important because it increases the information content available from either sensor alone; (3) The LUT climatology includes values as well as associated uncertainties in retrievals of R_{eff}, S and V. That is, the LUT algorithm propagates the error bars on the measured extinction ratios to corresponding error bars in retrieved parameters; (4) Retrieved parameters include an altitude- and time-dependent correction for any bias resulting from the assumption of a unimodal lognormal size distribution; and, (5) Unlike most previously produced stratospheric aerosol data sets, the LUT derived data set includes information about the aerosol size distribution width σ_g.

[60] **Acknowledgments.** This research was supported by NASA's Atmospheric Chemistry Modeling and Analysis Program through a SAGE II Science Team grant. The Cryogenic Limb Array Etalon Spectrometer (CLAES) absorption data were produced and distributed by the Upper Atmosphere Research Satellite (UARS) Project and the Distributed Active Archive Center at the Goddard Space Flight Center, Greenbelt, Maryland, respectively. These activities were sponsored by NASA's Mission to Planet Earth Program. The Stratospheric Aerosol and Gas Experiment II (SAGE II) extinction data were developed by NASA Langley Research Center and processed at the NASA LaRC Aerosol Research Branch. We appreciate unpublished data sets supplied to us by Terry Deshler. John Livingston's guidance and assistance is greatly appreciated as is technical support by Stephanie Ramirez.

References

Bauman, J. J., Stratospheric aerosol climatology derived from satellite solar occultation and infrared emission measurements, Ph.D. dissertation, 237 pp., State Univ. of New York, Stony Brook, 2000.

Bauman, J. J., P. B. Russell, M. A. Geller, and P. Hamill, A stratospheric aerosol climatology from SAGE II and CLAES measurements: 1. Methodology, *J. Geophys. Res.*, *108*, doi:10.1029/2002JD002992, in press, 2003.

Bluth, G. J. S., S. D. Doiron, C. C. Schnetzler, A. J. Krueger, and L. S. Walter, Global tracking of the SO_2 clouds from the June, 1991 Mount Pinatubo eruptions, *Geophys. Res. Lett.*, *19*, 151–154, 1992.

Bluth, G. J. S., W. I. Rose, I. E. Sprod, and A. J. Krueger, Stratospheric loading of sulfur from explosive volcanic eruptions, *J. Geol.*, *105*, 671–684, 1997.

Brewer, A. M., Evidence for a world circulation provided by the measurement of helium and water vapor distribution in the stratosphere, *Q. J. R. Meteorol. Soc.*, *75*, 351–363, 1949.

Brogniez, C., and J. Lenoble, Size distribution of stratospheric aerosols from SAGE II multi-wavelength extinctions, in *Aerosol and Climate*, edited by P. V. Hobbs and M. P. McCormick, pp. 305–311, A. Deepak, Hampton, Va., 1988.

Deshler, T., D. J. Hofmann, B. J. Johnson, and W. R. Rozier, Balloonborne measurements of the Pinatubo aerosol size distribution and volatility at Laramie, Wyoming during the summer of 1991, *Geophys. Res. Lett.*, *19*, 199–202, 1992.

Deshler, T., B. J. Johnson, and W. R. Rozier, Balloonborne measurements of Pinatubo aerosol during 1991 and 1992 at 41 N: Vertical profiles, size distribution, and volatility, *Geophys. Res. Lett.*, *20*, 1435–1438, 1993.

Dobson, G. M. B., Origin and distribution of polyatomic molecules in the atmosphere, *Proc. R. Soc. London, Ser. A*, *236*, 187–192, 1956.

Doiron, S. D., G. J. S. Bluth, C. C. Schnetzler, A. J. Krueger, and L. S. Water, Transport of Cerro Hudson SO_2 clouds, *Eos Trans. AGU*, *72*(45), 489, 498, 1991.

Evans, W. F. J., and J. B. Kerr, Estimates of the amount of sulfur dioxide injected into the stratosphere by the explosive volcano eruptions: El Chichon, Mystery Volcano, Mt. St. Helens, *Geophys. Res. Lett.*, *10*, 1049–1052, 1983.

Grainger, R. G., A. Lambert, C. D. Rodgers, F. W. Taylor, and T. Deshler, Stratospheric aerosol effective radius, surface area and volume estimated from infrared measurements, *J. Geophys. Res.*, *100*, 16,507–16,518, 1995.

Hamill, P., O. B. Toon, and C. S. Kiang, Microphysical processes affecting stratospheric aerosol particles, *J. Atmos. Sci.*, *34*, 1104–1119, 1977.

Hervig, M. E., T. Deshler, and J. M. Russell III, Aerosol size distributions obtained from HALOE spectral extinction measurements, *J. Geophys. Res.*, *103*, 1573–1584, 1998.

Hitchman, M., M. McKay, and C. R. Trepte, A climatology of stratospheric aerosol, *J. Geophys. Res.*, *99*, 20,689–20,700, 1994.

Hofmann, D. J., Stratospheric cloud micro-layers and small-scale temperature variations in the Arctic in 1989, *Geophys. Res. Lett.*, *17*, 369–372, 1990.

Hofmann, D. J., and T. Deshler, Stratospheric cloud observations during formation of the Antarctic ozone hole in 1989, *J. Geophys. Res.*, *96*, 2897–2912, 1991.

Hofmann, D. J., and J. M. Rosen, Stratospheric sulphuric acid mass fraction and mass estimate for the 1982 volcanic eruption of El Chichón, *Geophys. Res. Lett.*, *10*, 313–316, 1983.

Jäger, H., and D. Hofmann, Mid-latitude lidar backscatter to mass, area, and extinction conversion model based on in situ aerosol measurements from 1980 to 1987, *Appl. Opt.*, *30*, 127–138, 1991.

Kent, G. S., and M. P. McCormick, SAGE and SAM II measurements of global stratospheric optical depth and mass loading, *J. Geophys. Res*, *89*, 5303–5314, 1984.

Kent, G. S., P.-H. Wang, M. P. McCormick, and K. M. Skeens, Multiyear measurements of upper tropospheric aerosol characteristics, *J. Geophys. Res.*, *100*, 13,875–13,900, 1995.

Krueger, A. J., L. S. Walter, C. C. Schnetzler, and S. D. Doiron, TOMS measurement of the sulfur-dioxide emitted during the 1985 Nevado-Del-Ruiz eruptions, *J. Volcanol. Geotherm. Res.*, *41*, 7–15, 1990.

Lambert, A., R. G. Grainger, J. J. Remedios, W. J. Reburn, C. D. Rodgers, F. W. Taylor, A. E. Roche, J. B. Kumer, S. T. Massie, and T. Deshler, Validation of aerosol measurements from the Improved Stratospheric and Mesospheric Sounder, *J. Geophys. Res.*, *101*, 9811–9830, 1996.

Lambert, A., R. G. Grainger, C. D. Rodgers, F. W. Taylor, J. L. Mergenthaler, J. B. Kumer, and S. T. Massie, Global evolution of the Mt. Pinatubo volcanic aerosols observed by the infrared limb-sounding instruments CLAES and ISAMS on the Upper Atmosphere Research Satellite, *J. Geophys. Res.*, *102*, 1495–1512, 1997.

McCormick, M. P., and R. E. Veiga, SAGE II measurements of early Pinatubo aerosols, *Geophys. Res. Lett*, *19*, 155–158, 1992.

McCormick, M. P., and P.-H. Wang, Satellite measurements of stratospheric aerosols, in *Transport Processes in the Middle Atmosphere*, edited by G.Visconti and R. Garcia, pp. 103–120, D. Reidel, Norwell, Mass., 1987.

McCormick, M. P., P. Wang, and L. Poole, Stratospheric aerosols and clouds, in *Aerosol-Cloud-Climate Interactions*, edited by P. V. Hobbs, pp. 205–222, Academic, San Diego, Calif., 1993.

Pinto, J. P., R. P. Turco, and O. B. Toon, Self-limiting physical and chemical effects in volcanic eruption clouds, *J. Geophys. Res.*, *94*, 11,165–11,174, 1989.

Pruppacher, H. R., and J. D. Klett, *Microphysics of Clouds and Precipitation*, D. Reidel, Norwell, Mass., 1980.

Rodgers, C. D., R. J. Wells, R. G. Grainger, and F. W. Tayor, Improved stratospheric and mesospheric sounder validation: General approach and in-flight radiometric calibration, *J. Geophys. Res.*, *101*, 9775–9794, 1996.

Russell, P. B., et al., Global to microscale evolution of the Pinatubo volcanic aerosol derived from diverse measurements and analyses, *J. Geophys. Res.*, *101*, 18,745–18,764, 1996.

Steele, H. M., and P. Hamill, Effects of temperature and humidity on the growth and optical properties of sulphuric acid water droplets in the stratosphere, *J. Aerosol Sci.*, *12*, 517–528, 1981.

Taylor, F. W., et al., Remote sensing of atmospheric structure and composition by pressure modulator radiometry from space: The ISAMS experiment on UARS, *J. Geophys. Res.*, *98*, 10,799–10,814, 1993.

Thomason, L. W., A diagnostic stratospheric aerosol size distribution inferred from SAGE II measurements, *J. Geophys. Res.*, *96*, 22,501–22,508, 1991.

Thomason, L. W., L. R. Poole, and T. Deshler, A global climatology of stratospheric aerosol surface area density deduced from SAGE II measurements: 1984–1994, *J. Geophys. Res.*, *102*, 8967–8976, 1997.

Trepte, C. R., and M. H. Hitchman, Tropical stratospheric circulation deduced from satellite aerosol data, *Nature*, *335*, 626–628, 1992.

Trepte, C. R., L. W. Thomason, and G. S. Kent, Banded structures in stratospheric aerosol distributions, *Geophys. Res. Lett.*, *21*, 2397–2400, 1994.

Wang, P.-H., M. P. McCormick, T. J. Swissler, M. T. Osborn, W. H. Fuller, and G. K. Yue, Inference of stratospheric aerosols composition and size distribution from SAGE II satellite measurements, *J. Geophys. Res.*, *94*, 8435–8446, 1989.

Wilson, J. C., et al., In situ observations of aerosol and ClO after the 1991 eruption of Mount Pinatubo: Effect of reactions on sulfate aerosol, *Science*, *261*, 1140–1143, 1993.

Young, R., H. Houben, and O. Toon, Radiatively forced dispersion of the Mt. Pinatubo volcanic cloud and induced temperature perturbations in the stratosphere during the first few months following the eruption, *Geophys. Res. Lett.*, *21*, 369–372, 1994.

Yue, G. K., A new approach to retrieval of aerosol size distributions and integral properties from SAGE II aerosol extinction spectra, *J. Geophys. Res.*, *104*, 27,491–27,506, 1999.

J. J. Bauman and P. B. Russell, Advanced Projects Branch, NASA Ames Research Center, Mail Stop 244-14, Moffett Field, CA 94035-1000, USA. (jbauman@mail.arc.nasa.gov; prussell@mail.arc.nasa.gov)

M. A. Geller, Institute for Terrestrial and Planetary Atmospheres, State University of New York at Stony Brook, Stony Brook, NY 11794-5000, USA. (marvin.geller@sunysb.edu)

P. Hamill, Department of Physics, San Jose State University, 1 Washington Square, San Jose, CA 95192, USA. (hamill@stratus.arc.nasa.gov)